eLife

Reviewed Preprint
v2 • March 25, 2025
Revised by authors

Reviewed Preprint
v1 • October 11, 2024

Neuroscience

Non-feature-specific elevated responses and feature-specific backward replay in human brain induced by visual sequence exposure

Tao He, Xizi Gong, Qian Wang, Xinyi Zhu, Yunzhe Liu, Fang Fang

Center for the Cognitive Science of Language, Beijing Language and Culture University, Beijing, China • Key Laboratory of Language Cognitive Science (Ministry of Education), Beijing Language and Culture University, Beijing, China • School of Psychological and Cognitive Sciences and Beijing Key Laboratory of Behavior and Mental Health, Peking University, Beijing, China • IDG/McGovern Institute for Brain Research, Peking University, Beijing, China • Chinese Institute for Brain Research, Beijing, China • Peking-Tsinghua Center for Life Sciences, Peking University, Beijing, China • Key Laboratory of Machine Perception (Ministry of Education), Peking University, Beijing, China

eLife Assessment

This **valuable** study investigates both online responses to, and offline replay of, visual motion sequences. Sophisticated EEG analyses provide **convincing** evidence for both feature-specific and non-specific sequence representations. These intriguing findings will be of interest to perception and learning researchers alike.

https://doi.org/10.7554/eLife.101511.2.sa3

Abstract

The ability of cortical circuits to adapt in response to experience is a fundamental property of the brain. After exposure to a moving dot sequence, flashing a dot as a cue at the starting point of the sequence can elicit successive elevated responses even in the absence of the sequence. These cue-triggered elevated responses have been shown to play a crucial role in predicting future events in dynamic environments. However, temporal sequences we are exposed typically contain rich feature information. It remains unknown whether the elevated responses are feature specific and, more crucially, how the brain organizes sequence information after exposure. To address these questions, participants were exposed to a predefined sequence of four motion directions for about 30 min, followed by the presentation of the start or end motion direction of the sequence as a cue. Surprisingly, we found that cue-triggered elevated responses were not specific to any motion direction. Interestingly, motion direction information was spontaneously reactivated, and the motion sequence was backward replayed in a time-compressed manner. These effects were observed even after brief exposure. Notably, no replay events were observed when the second or third motion direction of the sequence served as a cue. Further analyses revealed that activity in the medial temporal lobe (MTL) preceded the ripple power increase in visual cortex at the onset

of replay, implying a coordinated relationship between the activities in the MTL and visual cortex. Together, these findings demonstrate that visual sequence exposure induces two-fold brain plasticity that may simultaneously serve for different functional purposes. The non-feature-specific elevated responses may facilitate general processing of upcoming stimuli, whereas the feature-specific backward replay may underpin passive learning of visual sequence.

Introduction

The capacity of cortical circuits to undergo plasticity in response to experience is a fundamental feature of the brain (Buonomano and Merzenich, 1998; Costandi, 2016; Li, 2016). This plasticity can be induced not only by active, task-dependent training, such as visual perceptual learning (Watanabe and Sasaki, 2015; Chen et al., 2016; Lu and Dosher, 2022), but also by passive, repetitive exposure (Gutnisky et al., 2009; Sasaki et al., 2010; Ekman et al., 2017). For instance, after repeated exposure to a moving dot sequence, flashing a dot (i.e., cue) at the starting point of the sequence elicits successive elevated neural responses in visual cortex, akin to those induced by the actual moving dot sequence in both humans (Ekman et al., 2017, 2023; Lu et al., 2020) and animals (Eagleman and Dragoi, 2012; Xu et al., 2012). This cue-triggered reactivation is thought to be driven by expectations and is prediction-related (Ekman et al., 2017, 2023), as it facilitates the prediction of upcoming stimuli and influences the perception of sensory information (Gutnisky et al., 2009; Baker et al., 2014; Pojoga et al., 2020).

Unlike the simple white dot sequences used in previous studies (Xu et al., 2012; Ekman et al., 2017, 2023; Lu et al., 2020), temporal sequences to which we are exposed in daily life usually contain rich feature information. However, it remains unknown whether cue-triggered elevated responses are feature-specific. On the one hand, if these responses are not feature-specific, they may reflect a general state of cortical readiness for any upcoming stimuli. On the other hand, if these responses are indeed specific to a particular feature in the sequence, they would selectively facilitate the processing of specific future events. This aligns with the view that expectation sharpens neural tuning and enhances the processing of expected stimuli (Kok et al., 2012). For instance, expectation has been shown to elevate the prestimulus baseline activity of sensory neurons tuned to expected stimuli (Wyart et al., 2012; Kok et al., 2014) and to preactivate stimulus templates in both the visual (Kok et al., 2017) and auditory (Demarchi et al., 2019) cortices. Notably, however, all these prediction-related, feature-specific activities were observed in static contexts. Whether prediction-related responses in dynamic temporal contexts (e.g., visual sequences) are feature-specific remains unclear.

After exposure to a feature-contained temporal sequence, another important question is how the feature information in the sequence is encoded and organized in neural activity following the cue. Previous studies have demonstrated that memory consolidation (Carr et al., 2011; Gridchyn et al., 2020; Gillespie et al., 2021) or learning process (Igata et al., 2021; Liu et al., 2021b, 2022) following training with a temporal sequence is associated with a neural phenomenon known as replay. Replay refers to the sequential reactivation of neural activity patterns associated with the trained sequence in both sleep (Lee and Wilson, 2002) and awake (Foster and Wilson, 2006) states. During replay, the neural representation of the trained sequence is temporally compressed and can occur in either a forward or backward direction (Carr et al., 2011; Joo and Frank, 2018; Nour et al., 2021; Liu et al., 2022; McFadyen et al., 2023). These replay events frequently coincide with sharp-wave ripples (SWRs), which are high-frequency (150–220 Hz) oscillations (O'Keefe and Nadel, 1978; Bush et al., 2022) detected in hippocampal local field potentials (Buzsáki, 1986, 2015). To date, replay has been observed in tasks involving sequences, such as nonlocal reinforcement learning (Liu et al., 2021b) and episodic memory retrieval (Wimmer et al., 2020). It remains unclear whether simple visual exposure to temporal sequences could also trigger replay events in humans.

In the current study, we used magnetoencephalography (MEG) to investigate whether cue-triggered elevated brain responses following visual sequence exposure are feature-specific and, more importantly, to determine how feature information in the exposed sequence is encoded and organized in the brain after exposure. To address these questions, participants were initially exposed to a predetermined motion sequence. We then decoded motion direction information during the blank period following the presentation of either the first or last motion direction in the sequence as a cue. Surprisingly, we found that cue-triggered elevated responses were not specific to any motion direction. Interestingly, motion direction information was spontaneously reactivated during the blank period, and the motion sequence was backward replayed in a time-compressed manner. This backward replay was identified even after brief exposure. However, neither forward nor backward replay was detected when an intermediate motion direction in the sequence was presented as a cue. Lastly, MEG source reconstruction analysis revealed that medial temporal lobe (MTL) activation preceded visual cortical activation, implying that the replay events observed in visual cortex may be triggered by activities in the MTL.

Results

The visual stimuli used in the study were four random-dot kinematograms (RDKs). All dots in an RDK moved in a single direction (i.e., 0°, 90°, 180°, or 270°) with 100% coherence. In Experiment 1, we included three trial conditions: full sequence trials, start-only trials, and end-only trials (**Figure 1A**). In a full sequence trial, participants were exposed to a predefined sequence of the four RDKs presented either clockwise (i.e., 0° → 90° → 180° → 270°) or counterclockwise at the center of the screen, with an inter-stimulus interval (ISI) of 300 ms between every two RDKs. In a start-or end-only trial, the first or last RDK of the sequence was presented at the beginning of the trial, followed by a blank period of 2.4 s. Participants were instructed to complete three successive phases: functional localizer phase, exposure phase, and main phase (**Figure 1B**). The functional localizer data were used to train models to decode each motion direction in the sequence. During this phase, one of the four RDKs was randomly presented for 1 s in each trial. During the exposure phase, participants were exposed only to full sequence trials for about 30 min. In the main phase, 50%, 25%, and 25% of all trials were full sequence, start- and end-only trials, respectively. The full sequence trials served as a topping-up exposure to maintain the exposure effect.

Cue-triggered elevated responses are not feature-specific

We first measured the event-related field (ERF) activity evoked by RDKs in the three trial conditions using all occipital gradiometer sensors (see Methods). **Figure 1C** shows the evoked responses for full sequence trials (left panel, cluster-based permutation test with a cluster forming threshold of $t > 3.1$ and 5000 permutations). Remarkably, start- and end-only trials elicited similar wave-like responses as the full sequence trials, despite the absence of stimuli following the first RDK (**Figure 1C**, middle and right panels, cluster-based permutation test with a cluster forming threshold of $t > 3.1$ and 5000 permutations). To further quantify the ERF peak amplitudes in the three conditions while mitigating baseline confounds, we calculated each peak amplitude using the 300 ms blank period just preceding the onset of the corresponding RDK as the baseline (see Methods). We found that the four successive RDKs in the full sequence trials evoked four comparable peaks after stimulus onset (**Figure 1C**, inset figure in the left panel; two-tailed t-test; all $ts_{(17)} > 6.8072$, all $ps < 10^{-5}$). Interestingly, in start- and end-only trials, significant peaks were still observed during the periods corresponding to the intervals of the second and third RDKs in the full sequence trials (**Figure 1C**, inset figures in the middle and right panels; start-only condition, two-tailed t-test; all $ts_{(17)} > 4.5790$, all $ps < 10^{-3}$; end-only condition, two-tailed t-test; all $ts_{(17)} > 6.0140$, all $ps < 10^{-4}$). However, no significant peak was observed during the period corresponding to the interval of the last RDK (start-only condition, two-tailed t-test; $t_{(17)} = 1.3221$, $p = 0.2036$; end-only condition, two-tailed t-test; $t_{(17)} = 0.2473$, $p = 0.8076$). These results demonstrate

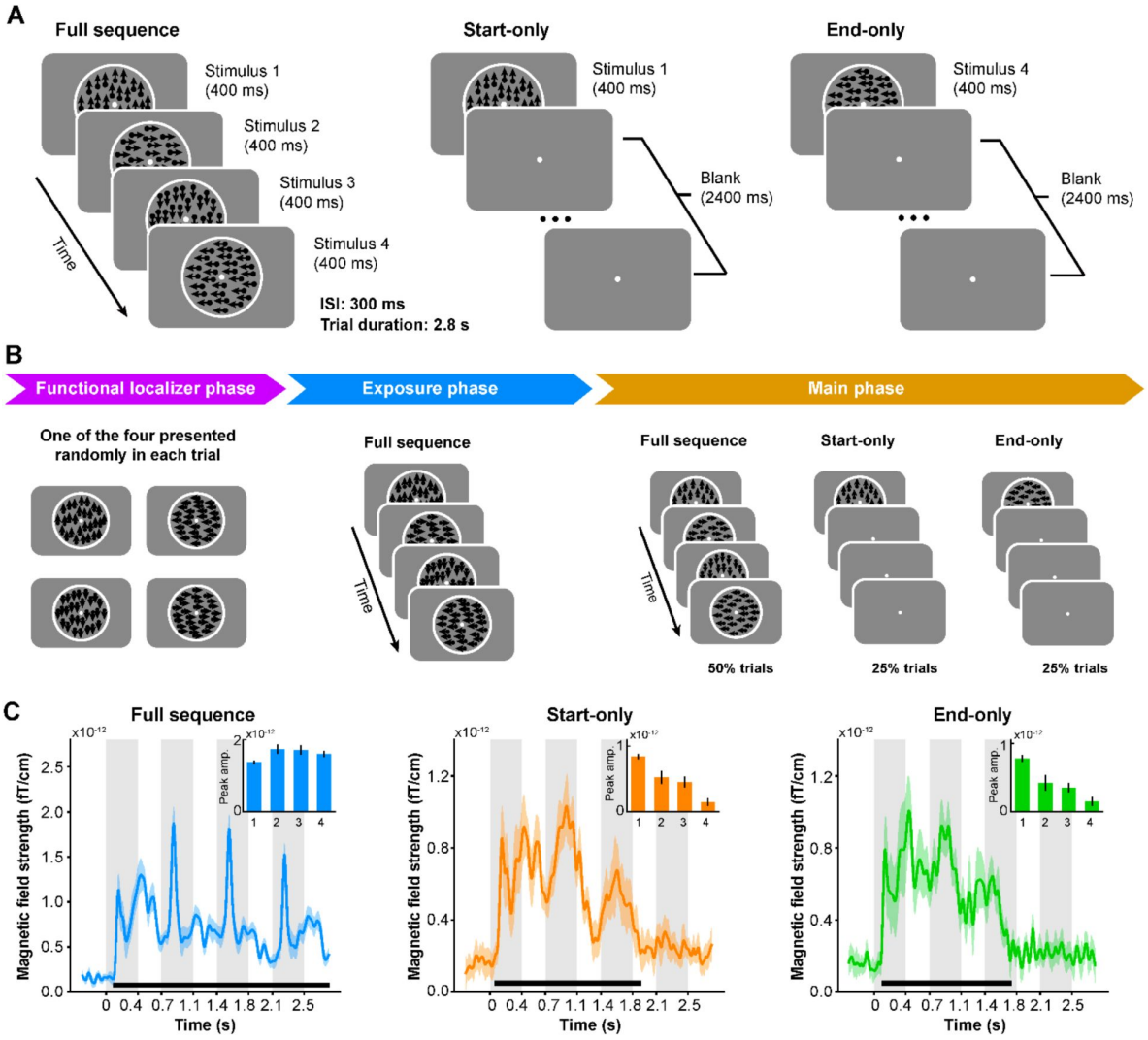

Figure 1.

Stimuli, experimental procedure and evoked responses in Experiment 1

(A) Participants were presented with RDKs in three conditions. In the full sequence trial condition, four successive RDKs were presented. In the start-or end-only condition, only the first or last RDK in the sequence was presented at the beginning of the trial. **(B)** During MEG scanning, the participants were presented with two functional localizer runs (i.e., functional localizer phase) before providing any sequence information. Next, they were exposed with four full sequence runs (i.e., exposure phase). Finally, in the main phase, full sequence, start- and end-only trials were presented in a pseudo-randomized order. **(C)** Evoked neural responses as a function of time relative to trial onset in the full sequence, start- and end-only trial conditions, respectively. Bold black lines at the bottom indicate temporal clusters in which they reached significance when compared to the pre-stimulus baseline. Inset figures at the top-right corner show the peak amplitudes during the four corresponding RDK intervals after baseline correction.

cue-triggered elevated neural responses following visual exposure to the RDK sequences, resembling previous studies using simple white dot sequences (Ekman et al., 2017; Lu et al., 2020).

Given that we observed elevated responses even in the absence of stimuli following the cue, we next examined whether these responses were specific to a particular feature (i.e., motion direction). Specifically, we asked whether motion directions could be successfully decoded in start- and end-only trials, particularly during the blank periods corresponding to the intervals of the second and third RDKs in full sequence trials. To this end, we applied a time-resolved decoding analysis. For each participant, we trained a one-versus-rest Lasso logistic regression model using the functional localizer data to classify the neural activity pattern elicited by each motion direction in the main phase. MEG signals from 72 occipital sensors were selected as features for the training model.

To validate the reliability of our model, we first used a leave-one-out cross-validation scheme on the localizer data to independently estimate decoding accuracy at each time point. At the group level, decoding accuracies peaked at 411 ms, 464 ms, 444 ms, and 434 ms after stimulus onset for motion directions 0° (55.37% ± 1.21), 90° (58.10% ± 1.14), 180° (54.07% ± 1.47), and 270° (53.64% ± 1.34), respectively. There were no significant differences among the four motion directions in terms of either latency ($F(3, 51) = 0.375$, $p = 0.7716$, $\eta_{p2} = 0.0159$) or decoding accuracy ($F(3, 51) = 2.757$, $p = 0.0517$, $\eta_{p2} = 0.091$) at the peak time point. Next, we trained a model using the localizer data averaged between 100 ms and 500 ms after stimulus onset. The trained model was then applied to the MEG signals recorded in the three trial conditions in the main phase. Finally, we calculated the decoding probability (Liu et al., 2019; Nour et al., 2021; Turner et al., 2023) for each motion direction at each time point at the group level (**Figure 2**). Here, decoding probability for each motion direction reflects the likelihood that the decoded stimulus had a specific motion direction at a given time point (see Methods). Therefore, it provides a time-resolved decoding preference for each motion direction, rather than only a single decoded label (e.g., 0°, 90°, 180°, or 270°).

In full sequence trials, the motion direction information could be successfully decoded, as evidenced by the highest decoding probability during the interval corresponding to the presentation of the respective RDK (**Figure 2A and 2B**, left panels). In start- and end-only trials, we could also reliably decode the motion direction of the first RDK (i.e., the cue) after stimulus onset (**Figure 2A and 2B**, middle and right panels, only the decoding probability of the first RDK surpass the peak-level significance threshold obtained from a nonparametric permutation test, FWE corrected across time). Surprisingly, however, subsequent motion direction information was absent at the group level during the post-cue blank period, where the cue-triggered elevated responses were previously observed (i.e., 0.4 – 2.8 s after stimulus onset). Together, these results demonstrate that the cue-triggered elevated response induced by visual sequence exposure was not consistently specific to a particular feature across participants and trials.

Time-compressed backward replay of exposed motion sequence

How is the motion direction information encoded and organized in the brain during the post-cue blank period? Clearly, the motion direction representation is not time-locked to the onset of the cue in either start-or end-only trials. However, it is possible that individual motion directions are encoded in the MEG signals in a spontaneous way but are sequentially organized (Liu et al., 2019).

To test this hypothesis, we trained four decoding models using the localizer data to capture the neural features of the four motion directions. We employed four decoding models because our aim was to build feature-specific classifiers, each sensitive to only one motion direction. These classifiers were designed to quantify the evidence of feature-specific sequence in subsequent

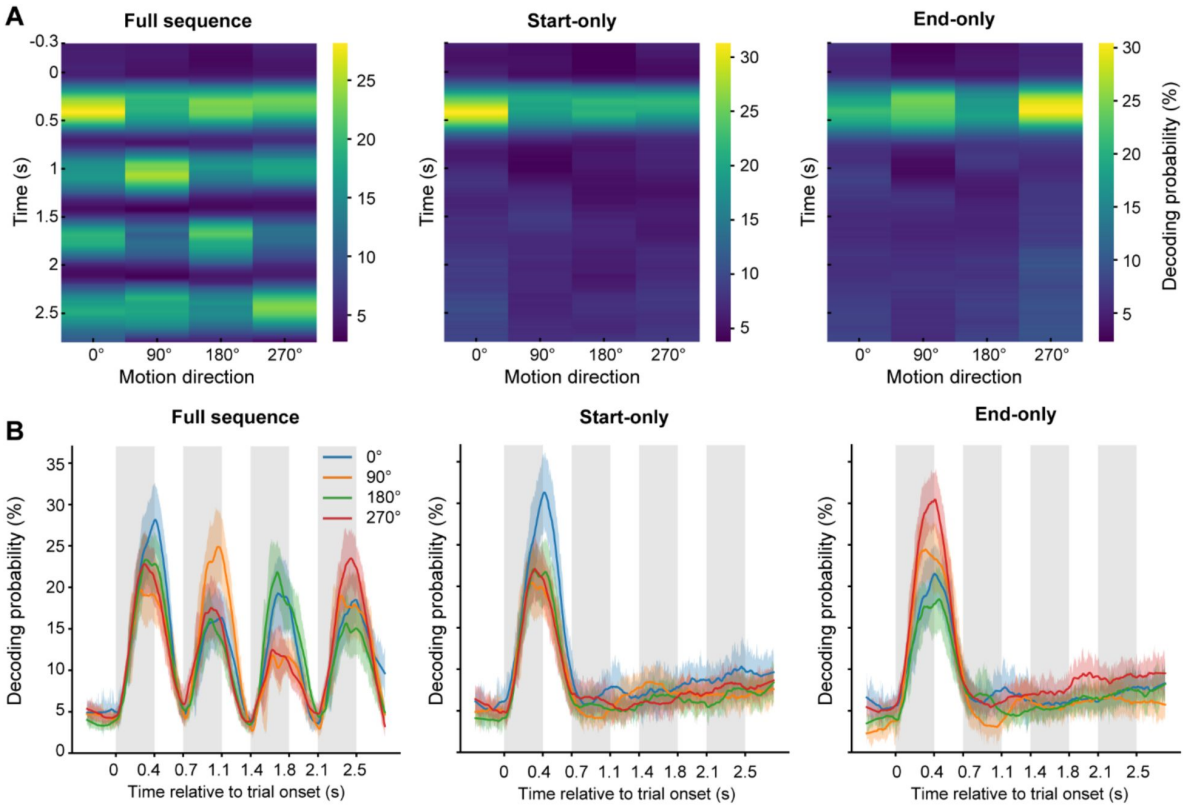

Figure 2.

Time-resolved decoding probability for each motion direction

(A) Visualization of the time-resolved decoding probability in the three trial conditions. Each row shows the decoding probabilities for the four motion directions at that time point and each column indicates one of the four motion directions. **(B)** The line plots of the time-resolved decoding probability for the three trial conditions. Each colored line shows the time course of the decoding probability for each motion direction. For the start- and end-only conditions, we calculated the permutation threshold estimated by randomly shuffling of the labels and re-decoding, only the decoding probability of the cue surpassed the threshold.

analyses. The models used a one-versus-rest Lasso logistic regression algorithm, with MEG signals from 72 occipital sensors as features (**Figure 3A**). For each participant and motion direction, we then selected the time point with the highest decoding accuracy, which was estimated during the validation of the functional localizer data, as the optimal time point. These optimal time points were chosen because they are believed to carry the richest feature information (Mo et al., 2019). For subsequent analyses, we obtained four classifiers that were trained on the localizer data at their respective optimal time points. Each classifier yielded significant decoding probability only when the stimulus matched the motion direction it was trained to detect (**Figure 3B**). We did not find any spatial correlation between any two trained classifiers (highest correlation $r < 0.12$, **Figure S1A**). Since the optimal time point varied across participants and motion directions, we circularly shifted the decoding probabilities over time and aligned them to a common time point (arbitrarily set to 200 ms after stimulus onset) for visualization at the group level (**Figure 3B**).

Having established the classifiers for each participant and motion direction, we then applied the classifiers to the MEG signals during the post-cue blank period in start- and end-only conditions to estimate the reactivation probability (i.e., decoding probability) for each motion direction at each time point (**Figure 3C**; Liu et al., 2019; Wimmer et al., 2020; Nour et al., 2021). Example trials for the start- and end-only conditions are shown in **Figure S2**. The results revealed that motion direction reactivations occurred sparsely during the post-cue blank period, rather than crowded within intervals corresponding to the RDK presentations in the full sequence condition, suggesting that motion direction information might be reactivated in a spontaneous way. Next, we applied temporally delayed linear modeling (TDLM) to quantify whether and how these spontaneous reactivations followed the order of the exposed sequence (**Figure 3D**). This algorithm includes two-level regression analyses; a first-level regression that quantify evidence for each pairwise transition (e.g., 0° → 90°), and a second-level regression that evaluates the extent to which reactivation patterns align with a particular order of interest. Finally, we defined "sequenceness" as a metric of forward (i.e., 0° → 90° → 180° → 270°) or backward (i.e., 270° → 180° → 90° → 0°) replay (Kurth-Nelson et al., 2016; Liu et al., 2019, 2021a; Nour et al., 2021).

As shown in **Figure 4A** and **4B**, in the start-only condition, we found evidence of backward replay of the exposed motion sequence (i.e., the replay sequence was 270° → 180° → 90° → 0° when the exposed motion sequence was 0° → 90° → 180° → 270°) during the post-cue blank period, with a peak transition lag at 28–40 ms (maximal effect at 32 ms-lag: $\triangle = -0.0202 \pm 0.002$, $p < 1/24 \triangle 0.042$, peak-level significance threshold derived from a nonparametric permutation test, FWE corrected across lags, **Figure 4B**). For visualization, an example of backward replay of the motion sequence is illustrated in **Figure 4A**. This effect was observed in most participants (**Figure S3A**). In the end-only condition, we also found evidence of backward replay during the post-cue blank period, with a peak transition lag at 28–36 ms (maximal effect at 32 ms-lag: $\triangle = -0.0145 \pm 0.0016$, $p < 1/24 \triangle 0.042$, peak-level significance threshold obtained from a nonparametric permutation test, FWE corrected across lags; **Figure 4E**). **Figure 4D** shows an example of backward replay of the motion sequence in this condition, found in most participants (**Figure S3A**). Note that the time lag in the horizontal axis in **Figure 4B** and **4E** indicates the interval between the onsets of every two items in the replayed motion sequence. We found that the replayed sequence was approximately 10 times faster than the evoked activity sequence in the full sequence condition.

To further examine the period during which the backward replay occurred most frequently, we divided the blank period (2.4 s) into 4 stages, each lasting 600 ms. In start-only trials, we found that the backward replay predominantly appeared within the third stage of the blank period (1.2 – 1.8 s after the onset of the blank period, Wilcoxon signed-rank test, $p = 0.0108$), but there was no significant sequenceness in the other three stages (first stage, $p = 0.7112$; second stage, $p = 0.5566$; fourth stage, $p = 0.6791$; **Figure 4C**). In end-only trials, the backward replay was more likely to occur during the second and third stages of the blank period, although the results approached, but did not reach, significance (Wilcoxon signed-rank test, second stage, $p = 0.0936$; third stage, $p =$

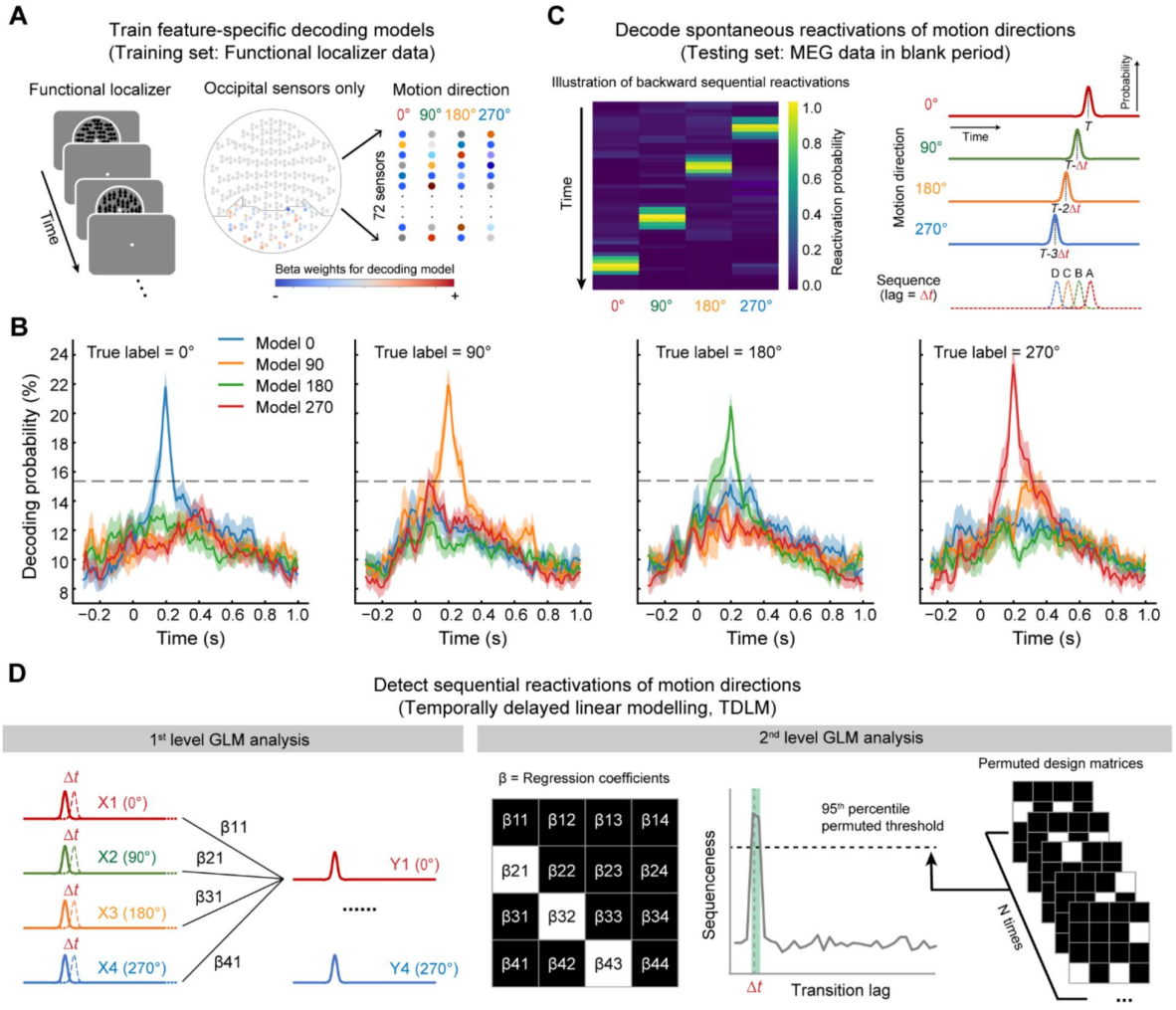

Figure 3.

Illustration of replay analysis pipeline: Temporally delayed linear modeling (TDLM)

(A) A Lasso logistic regression model was trained for each participant and motion direction using MEG signals from the functional localizer data. **(B)** The four feature-specific models that were trained using functional localizer data. The decoding probabilities were aligned at 200 ms post-stimulus onset according to their corresponding optimal time point per participant and motion direction. Each colored line indicates the decoding results of a model applied to a motion direction dataset. The dashed horizontal line indicates the permutation threshold estimated by random shuffling of the labels and re-decoding. **(C)** The four models were next applied to MEG signals during the post-cue blank period to derive a decoded reactivation matrix [time x motion direction]. An illustration of backward sequential reactivations of motion direction is shown on the left. Reactivation probabilities correspond to the decoding probabilities derived from the four models. **(D)** Using TDLM, we quantified the evidence for sequential replay of the motion sequence during the post-cue blank period in start- and end-only conditions. We initially performed a time-lagged regression to create a [4 x 4] regression coefficient matrix for each time lag by regressing each lagged predictor matrix X(△t) onto the original reactivation matrix, Y (i.e., 1st level GLM analysis). The degree to which the reactivations systematically follow a transition matrix of interest was measured by "sequenceness" (i.e., 2nd level GLM analysis). We tested the magnitude of this sequenceness at each time lag independently for all transition lags up to 600 ms. The dashed line represents the corrected nonparametric statistical significance threshold (see Methods). The green area indicates the lags when the evidence of sequenceness in the backward direction exceeded the permutation threshold.

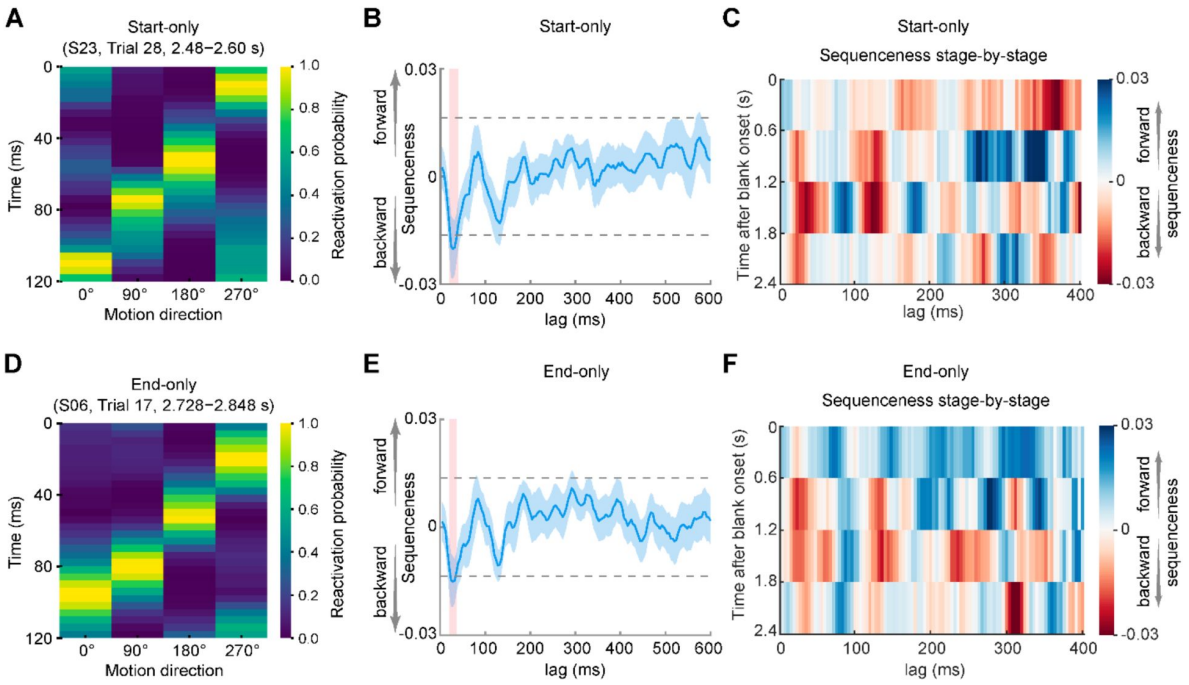

Figure 4.

Backward replay in both start- and end-only conditions

(A and **D)** Examples of backward sequential reactivation in start-(A) and end-(D) only conditions from a representative participant. Each row represents the reactivation probabilities for the four motion directions at that time point and each column indicates one of the four motion directions. **(B and E)** Backward replay of the exposed motion sequence with peak transition lags at 28–40 ms in the start-only condition (B) and at 28 – 36 ms in the end-only condition (E). Horizontal dashed lines represent corrected significance levels from a nonparametric permutation test at the 2nd-level GLM analysis of TDLM. **(C and F)** Backward replay of the exposed motion sequence predominantly appeared at 1.2 – 1.8 s in the start-only condition (C) and 0.6 – 1.8 s in the end-only condition (F) after the onset of the blank period.

0.0642; **Figure 4F**), In contrast, the replay was not frequently observed during the first and last stages (Wilcoxon signed-rank test, first stage, p = 0.9479; fourth stage, p = 0.4997). Finally, in a control analysis, we conducted a comprehensive examination of all 24 potential sequences. Only the backward replay was detected in both start- and end-only conditions (**Figure S4**).

Backward replay is cue-dependent and depends on the amount of exposure

So far, we have demonstrated that the cue-triggered elevated responses induced by the motion sequence exposure were not motion direction specific. However, motion information was spontaneously reactivated and the motion sequence was backward replayed in a time-compressed manner. It remains unknown whether the observed backward replay of the motion sequence was cue-dependent. In other words, does the replay of the motion sequence occur irrespective of which item of the sequence is presented as a cue? To address this question, we conducted Experiment 2, mirroring the design of Experiment 1 but with a different cue. Instead of flashing the first or last RDK, we presented the second or third RDK as a cue (2^{nd}-only or 3^{rd}-only condition, see **Figure S5A** and Methods) to examine whether these two non-terminal cues could induce replay during the post-cue blank period. We found no evidence of either forward or backward replay in either condition (**Figure 5A**; maximal nonsignificant effect at 32 ms-lag: 2^{nd}-only condition, $\beta = -0.0024 \pm 0.0014$; 3^{rd}-only condition, $\beta = -0.0018 \pm 0.0015$).

Another interesting question is how varying the amount of exposure would affect replay events during the blank period. To explore this issue, we conducted Experiment 3, also similar to Experiment 1 except for the removal of the exposure phase. Accordingly, only full sequence trials (50% trials) in the main phase served for exposure (see **Figure S5B** and Methods). In the start-only condition, we found a numerical trend of backward replay at transition lags at 20–40 ms, although it did not reach statistical significance (**Figure 5B**, left panel; maximum effect at 28 ms-lag: $\beta = -0.0139 \pm 0.0021$). In the end-only condition, the evidence for backward replay just reached the significance level at transition lags at 20 – 40 ms (**Figure 5B**, right panel; maximal effect at 24 ms-lag: $\beta = -0.0147 \pm 0.0019$, $p < 1/24 \approx 0.042$, using the peak-level significance threshold from a nonparametric permutation test, FWE-corrected across lags).

Power increase in replay-associated sharp-wave ripple frequencies

Previous studies on rodents and humans showed that replay events are associated with increased high-frequency ripple power (Buzsáki, 2015; Liu et al., 2019). To investigate whether such replay-associated power increase could be observed in our study, we performed a time-frequency analysis using combined data from the start- and end-only conditions in Experiment 1. We first identified putative replay onsets during the post-cue blank period in each trial. Replay onsets were determined by choosing time points with a high (>95^{th} percentile) probability for backward replay with a 32 ms-lag transition (maximal replay effect at the group level for both start- and end-only conditions, **Figure 4B** and **4E**; see Methods for details). Using the MEG signals recorded from whole brain sensors, we found a transient ripple power increase at 120–180 Hz at the onset of replay events, compared to the baseline period of 50–100 ms prior to replay onset (**Figure 6A**; cluster-based permutation test with cluster forming threshold t > 3.1 and 5000 permutations).

Visual cortical activation lags MTL activation

Since replay events were obtained based on decoding probabilities of motion directions from occipital sensors only, we next examined whether the observed replay onsets were related to power increase within visual cortex. Using a linearly constrained minimum variance (LCMV) beamforming algorithm (Van Veen et al., 1997), we first epoched the data using replay onsets combined from both start- and end-only conditions and then beamformed the broadband power into the source space (see Methods). We found that the power increase at replay onset was

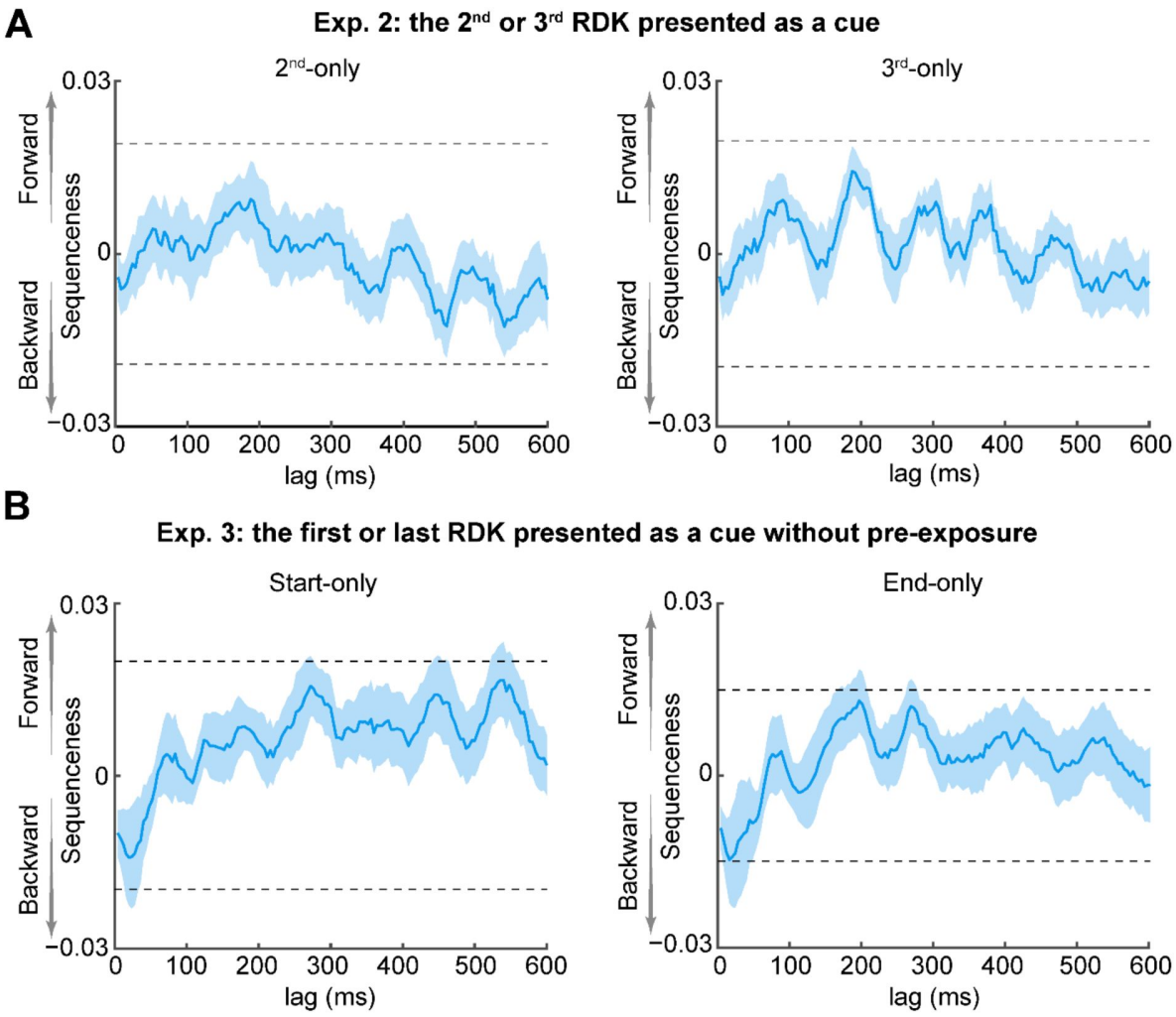

Figure 5.

Backward replay is cue-dependent and depends on the amount of exposure

(A) No evidence for replay was found in either the 2nd-only (left) or 3rd-only (right) condition in Experiment 2. Horizontal dashed lines have the same meaning as those in **Figure 4B and 4E**. **(B)** In Experiment 3, immediately after the functional localizer phase, participants entered the main phase without the exposure phase. In the end-only condition, backward replay was observed; however, in the start-only condition, no such replay was observed.

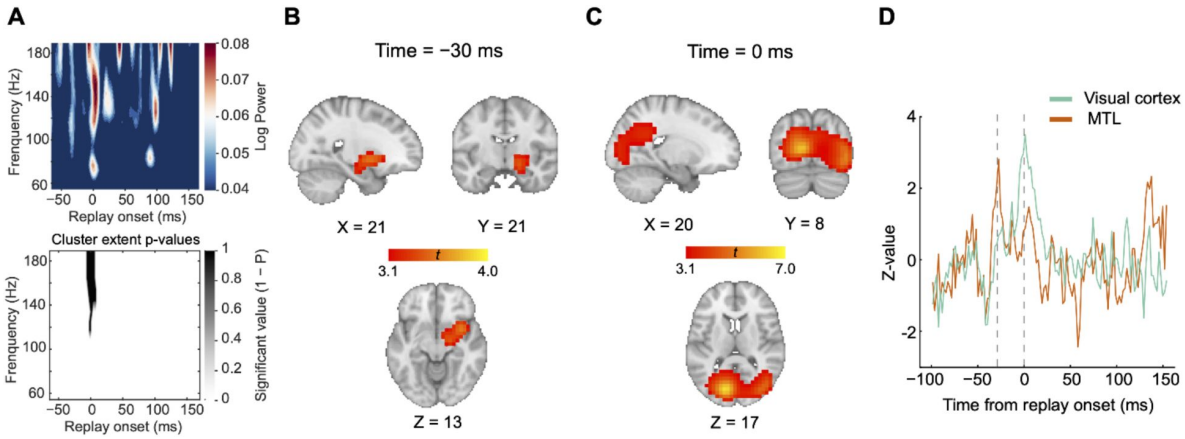

Figure 6.

Replay events align with ripple power, with source activation in the MTL preceding activation in visual cortex

(A) Top: In Experiment 1, a time-frequency decomposition of sensor-level data revealing a brief increase in high-frequency oscillatory power at replay onset. Bottom: a cluster-based permutation test (cluster forming threshold, t > 3.1; number of permutations = 5000) could identify a significant cluster around 140 Hz. **(B)** Source localization of ripple-band power 30 ms before replay onset showing significant activation in the MTL (peak Montreal Neurological Institute [MNI] coordinates: X = 21, Y = 21, Z = 13. Neurological orientation.) **(C)** Source localization of ripple-band power at replay onset showing significant activation in visual cortex (peak MNI coordinates: X = 20, Y = 8, Z = 17). **(D)** The activation time course of the MTL at its peak MNI coordinate is shown in red, whereas that of visual cortex at its peak MNI coordinate is displayed in green. The MTL reached its peak activation before visual cortex.

localized to sources in bilateral visual cortex (**Figure 6C**). Moreover, the right MTL, including the hippocampus and amygdala, was associated with power increase prior to the onset of replay events (**Figure 6B**). Specifically, activation (i.e., power increase) in the MTL occurred 30 ms earlier than that in visual cortex ($p < 0.05$, corrected, whole brain nonparametric permutation test). For display purposes, we extracted activations from the 10 most activated voxels within the MTL and visual cortex, respectively, and plotted the time courses of their broadband power. Peak activation in visual cortex at replay onset was preceded by peak activation in the MTL (**Figure 6D**), implying an information flow from the MTL to visual cortex.

Discussion

We found the co-existence of time-locked, non-feature-specific elevated responses and non-time-locked, feature-specific backward replay after visual sequence exposure in human brain. The feature-specific backward replay occurred in a time-compressed manner and could be triggered only by the first or last stimulus of the sequence. Interestingly, even brief exposure to the sequence could still induce a trend for the backward replay. Finally, we observed that MTL activity preceded the ripple power increase in visual cortex at replay onset.

Our study provides two new findings in the fields of vision and learning. First, different from many previous studies showing that expectation-based responses in static contexts are feature-specific (Wyart et al., 2012; Kok et al., 2014, 2017), we show here that prediction-related elevated responses in the dynamic temporal context are not. This non-feature-specific elevated responses potentially facilitate the general processing of any upcoming stimuli, rather than stimuli with a specific feature. Second, contrary to the prevailing notion that replay in learning and memory requires lengthy training with a task, our study shows that even brief exposure to a visual sequence is sufficient to induce replay. The replay we unveiled here may play a critical role in memorizing the visual sequence.

Regarding the two-fold neural consequences following the visual sequence exposure, the non-feature-specific elevated responses could be induced by rhythmic entrainment. Substantial evidence supports that rhythmic stimulation can entrain neural oscillations, which in turn facilitates predictions about future inputs and enhances the brain's readiness for incoming stimuli (Lakatos et al., 2008, 2013; Herrmann et al., 2016; Barne et al., 2022). For instance, recent findings demonstrate that even task-irrelevant information could be more effectively decoded when presented at moments close to a highly probable target presentation (Auksztulewicz et al., 2019). In our study, the rhythmic presentation of the motion sequence may have entrained oscillatory activity in the brain, leading to periodic activation of sensory cortices. This rhythmic entrainment likely serves as a possible mechanism supporting the general facilitation of neural processing for any upcoming stimuli, independent of specific stimulus features.

In contrast, feature-specific replay may operate through a different mechanism driven by intrinsic neural processes rather than direct external stimuli. Therefore, this intrinsic activity is not time-locked to stimulus onset, but instead manifests in a spontaneous way. Furthermore, since replay often occurs during offline periods (e.g., rest or blank period), it allows the neural system to reactivate and consolidate past experiences without interference from ongoing external inputs. As a result, feature-specific replay may facilitate the integration of fragmented experiences into coherent representations, thereby subserving visual sequence learning and memory.

Another interesting question regarding the two-fold neural responses is whether the elevated responses and the backward replay share the same neural origin, for instance, originating from the hippocampus or other brain areas. For the elevated responses, the cue serves to provide temporal information for upcoming stimuli but without detailed feature information, thereby priming the cortices for activation and facilitating the general processing of future events.

Previous animal studies (Xu et al., 2012; Gavornik and Bear, 2014) showed that this process can be implemented through a simple local synaptic mechanism in visual cortex (Xu et al., 2012) without top-down guidance. Moreover, Ekman et al. (2023) recently found no functional relationship between activities in V1 and the hippocampus when exposing human participants with a white dot sequence, further suggesting that the elevated responses may indeed originate in visual cortex.

Different from the elevated responses, the replay events are likely initiated by the hippocampus. This speculation is supported by two key findings. First, the replay of the motion direction information manifested in a backward direction and a time-compressed manner. Second, the replay is observed regardless of whether the cue is the first or last RDK in the sequence. Both of these two properties cannot be explained by a simple local synaptic mechanism (Xu et al., 2012) or a pattern completion-like mechanism (Hindy et al., 2016; Ekman et al., 2017; Kok and Turk-Browne, 2018) within visual cortex alone. Instead, the replay entails reorganizing the motion direction sequence in the brain. Therefore, we propose the involvement of active communication between the hippocampus and visual cortex in the occurrence of replay events, consistent with the view that the hippocampus encodes relationships among stimuli whereas visual cortex primarily acts as a platform for the manifestation of replay events (Whittington et al., 2020). Previous studies on memory consolidation considered the exchange of information between these two regions critical for facilitating replay events through hippocampal-neocortical circuits (Buzsáki, 1996; Ji and Wilson, 2007; Carr et al., 2011; Ólafsdóttir et al., 2016; Buch et al., 2021). Functionally, replay events offer a mechanism for transferring recent experience from the hippocampus to the cortex, enabling the encoding of stimulus relationships in the cortex (Marr and Brindley, 1971; Alvarez and Squire, 1994; Redish and Touretzky, 1998; Dimakopoulos et al., 2022).

A natural behavioral consequence of visual sequence exposure is visual sequence learning (Baker et al., 2014; Finnie et al., 2021; Ekman et al., 2023). How is the learning implemented through hippocampus-dependent replay in visual cortex? Three key processes are considered here. First, the hippocampus is involved in encoding relationships among stimuli (Staresina and Davachi, 2009; Turk-Browne et al., 2009; Hsieh et al., 2014; Garvert et al., 2017); in fact, the ability to encode such relationships drastically decreases when the hippocampus is damaged (Chun and Phelps, 1999; Hannula et al., 2006; Konkel et al., 2008; Schapiro et al., 2014; Finnie et al., 2021). Second, visual cortical areas act as a “cognitive blackboard” where task-relevant features are highlighted through feedback connections (Roelfsema and de Lange, 2016). Such a blackboard can be flexibly written or edited. Third, there are strong bidirectional connections between the hippocampus and sensory cortices (Eichenbaum et al., 2007; Henke, 2010). As proposed by the hippocampal-cortical backward projection model (Rolls, 2000), sequential reactivations of feature information initially generated in the hippocampus can be quickly and accurately sent back to the sensory cortices, consistent with the findings of Ji and Wilson, (2007). A recent study also provided direct evidence that visual sequence plasticity is impaired when the hippocampus is damaged (Finnie et al., 2021), supporting the hypothesis of functional feedback information flow.

Why does the replay manifest in a reverse order? To date, there is no consensus on this issue. In rodents, a seminal study of replay during the awake state showed that when animals stopped at the end of a rewarded pathway, place cells were reactivated in the reverse order of the previously experienced direction (Foster and Wilson, 2006). However, a later study revealed that awake replay could occur in either a forward or backward direction relative to behavioral experience (Diba and Buzsáki, 2007). Similarly, in humans, both directions have been observed in different nonspatial cognitive tasks (Liu et al., 2019, 2021b; Wimmer et al., 2020). Forward replay may be associated with planning (Ólafsdóttir et al., 2015; Gillespie et al., 2021), providing information pertaining to the assessment of future pathways (Diba and Buzsáki, 2007). Backward replay may be more related to experience, as often observed at the end of runs when

animals consume a reward (Foster and Wilson, 2006; Ambrose et al., 2016). Nevertheless, the exact function of the replay direction remains mysterious, as both forward and backward replays are modulated by task demands (Ólafsdóttir et al., 2017). Thus, the underlying neural mechanisms of backward replay in visual cortex remain to be investigated.

Finally, we also found that replay occurrence is modulated by the cue. This result highlights the importance of the start and end points of the sequence in the replay. One fascinating proposal is that the replay event is sensitive to sequence boundaries, as indicated by the role of the start or end point of the sequence as salient boundaries that anchor place cell firing (Rivard et al., 2004). Accordingly, previous studies have shown that when rats are trained to run along a linear track starting at different points, place fields tend to be anchored to either the start or end of the journey (Gothard et al., 1996; Redish et al., 2000), suggesting that a boundary is essential to sequence integrity and may play a pivotal role in triggering replay onset. An alternative explanation to these findings posits that the onset of the second or third stimulus in the sequence reinstate the neural representations of a partial visual sequence (Ekman et al., 2023). For example, for a given sequence, A → B → C → D, flashing the third stimulus (i.e., C) only trigger a backward reactivation of the sequence giving C → B → A during the blank period.

Taken together, we found that simple visual sequence exposure could concurrently induce two-fold brain plasticity, that is, non-feature-specific elevated responses and feature-specific backward replay in the human visual cortex. We speculate that the non-feature-specific elevated responses may enhance general processing of upcoming visual stimuli, whereas the feature-specific backward replay may subserve visual sequence learning and memory. These findings significantly advance our understanding of the task-independence and the multifaceted nature of brain plasticity in response to visual experience.

Methods

Participants

A total of 59 healthy participants (29 females) were involved in the three experiments (Experiment 1: n = 21, 11 females, 22.1 ± 2.61 years; Experiment 2: n = 18, 10 females, 23.56 ± 3.29 years; Experiment 3: n = 20, 10 females, 20.65 ± 2.62 years). In Experiment 1, data from three participants were excluded before analyses, as two showed large head motion (>20 mm) and the behavioral performance of one was at chance level. In Experiment 3, data from two participants were excluded before analyses because of large head motion (>20 mm). All participants were recruited in exchange for monetary compensation (100 RMB/h). They reported normal or corrected-to-normal vision and had no history of neurological disorders. They were naive to the purposes of the study. The experiments reported here were carried out in accordance with the guidelines expressed in the Declaration of Helsinki. All participants provided written informed consent in accordance with the procedures and protocols approved by the Human Subject Review Committee of Peking University.

Task

Experiment 1

Visual stimuli were RDKs with 100% coherence. All dots in an RDK moved in the same direction (luminance: 2.86 cd/ m^2; diameter: 0.1°; speed: 8°/s) and were presented against a gray background (luminance: 16.7 cd/m^2). At any one moment, 400 dots were visible within a 9° circular aperture and moved in one of the four directions: 0° (right), 90° (up), 180° (left), and 270° (down). Each participant completed three phases successively in the MEG scanner, namely, the functional localizer phase, the exposure phase, and the main phase (**Figure 1C**). In the functional localizer

phase, each trial started with the presentation of an RDK for 1 s followed by a 1–1.5 s intertrial interval (ITI). Participants did not need to perform any task in this phase. The motion direction of the RDK was randomly chosen from the four directions. Each participant performed two functional localizer runs and, each run comprised 100 trials, resulting in a total of 50 trials per motion direction. The localizer data were used to train motion direction classifiers. This phase took approximately 10 min.

In the exposure phase, we showed participants the four RDKs in either clockwise or counterclockwise order (e.g., 0° → 90° → 180° → 270°, **Figure 1A** and **1C**); each was displayed for 400 ms, followed by 300 ms of a blank screen with a fixation only. Therefore, the full sequence lasted for 2.8 s. The order was counterbalanced among participants, but once decided, it was fixed for each participant. Participants were instructed to detect an oddball RDK by pressing a button, i.e., in 20% trials, dots in one of the four RDKs traveled at a faster speed (9°/s). Each participant completed four runs of 50 trials.

In the main phase, participants were presented with trials in three different conditions: full sequence condition (50% trials), start-only condition (25% trials), and end-only condition (25% trials). Trials in the full sequence condition were identical to those in the exposure phase which served as "topping-up" exposure to maintain the exposure effect, similar to "topping-up" adaptation in visual adaptation studies (Fang et al., 2005). In the start- and end-only conditions; however, we only presented the first RDK (start-only condition) or the last RDK (end-only condition) of the full sequence. For a given run, the order of the three conditions was pseudorandomized with the restriction that the start- and end-only trials were always preceded or followed by a full sequence trial. Participants performed an identical oddball detection task as during the exposure phase. The oddball occurred only in 10% of full sequence trials. Finally, each participant completed four runs of 48 trials, yielding a total of 96 full sequence trials, 48 start-only trials, and 48 end-only trials.

Experiments 2 and 3

In Experiment 2, we only presented the second or third RDK as a cue at the start of the trial, referred to as the 2^{nd}-only and 3^{rd}-only conditions, respectively. The procedure of Experiment 2 was similar to that of Experiment 1 except that the start- and end-only conditions were replaced with the 2^{nd}-only and 3^{rd}-only conditions. Experiment 3 followed the same procedure as Experiment 1 except that the exposure phase was removed.

Quantification and statistical analysis

MEG acquisition and preprocessing

Neuromagnetic signals were recorded continuously at 1000 Hz with a 306-channel (204 planar gradiometers; 102 magnetometers), whole-head MEG system (Elekta Neuromag TRIUX) in a magnetically shielded room. Before scanning, four-headed position indicator coils attached to the scalp determined the head position with respect to the sensor array. Coil location was digitized with respect to three anatomical landmarks (nasion and preauricular points) with a 3D digitizer (Polhemus Isotrak system). Participants sat upright inside the scanner, while the stimuli were projected onto a screen suspended in front of them. Participants responded using a MEG-compatible button box held in their right hand.

To reduce noise from external environment, the temporal extension of signal-space separation (tSSS) method was applied at the preprocessing stage using the Elekta Neuromag MaxFilter software (Taulu and Simola, 2006). MEG signals were high-pass filtered at 0.5 Hz using a first-order IIR filter to remove slow-drifts. Data were then downsampled from 1000 Hz to 250 Hz for

sequenceness analysis or 500 Hz for time-frequency analysis. Excessively noisy segments and sensors were automatically removed before independent component analysis (FastICA, *http://research.ics.aalto.fi/ica/fastica*) and performed to remove artifacts including cardiac signals, eye movements and blinks, and environmental noise. Artifact components were removed by visual inspection of spatial topography, time course, kurtosis of the time course, and frequency spectrum of all components. Only 72 sensors (including both gradiometers and magnetometers) covering the occipital lobe, labeled as "Occipital" in the MEG data acquisition system were used for MEG data analyses, except for source localization. The sensor selection was primarily motivated by the main objective of the study, examining replay events in visual cortex.

Event-related fields

To calculate the event-related fields (ERFs), MEG epochs were segmented around trial onset for each trial and baseline-corrected using the mean activity in the time window of [−0.3 s, 0] before trial onset. Only 48 planar gradiometers of "Occipital" sensors were used to calculate the ERFs. The planar-combined ERF activity was then averaged for each condition. To minimize potential baseline confounds caused by the short interval between ev ery two RDKs, we further calculated the ERF peak amplitude using the mean activity in the time window of [−0.3 s, 0] before the onset of the corresponding RDK as the baseline. Subsequently, peak amplitude during each of the four RDK intervals was calculated as the difference between the peak and its corresponding baseline.

Multivariate pattern analyses

Multivariate pattern analyses (MVPA) were performed to classify the neural activity patterns elicited by the motion directions of the four RDKs in the main phase. A one-versus-rest Lasso-regularized logistic regression model was trained using the MEG signals from the 72 occipital sensors in the functional localizer phase. Specifically, we trained a five-class classifier, including four classes from trials in which the four RDKs were presented, and an additional class comprising an equivalent amount of null data extracted from the 1–1.5 s ITI. Null data were included to reduce the spatial correlation among the classes, thereby concurrently lowering the decoding probabilities for all classes (Liu et al., 2021a; Nour et al., 2021). Class weights were balanced by adjusting inversely proportional to class frequencies (i.e., trial numbers) in the training procedure. To reduce noise, MEG signals were averaged across every five trials within the same class before decoding.

The trained classifier was then applied to MEG signals at each time point in the main phase, and decoding probabilities were computed as the outputs of the classifier. Different from the conventional decoding accuracy, where the classifier predicts a single label at each time point, decoding probabilities provide a likelihood estimate for each class. In our study, the classifier outputs a 5-column matrix for all trials, where each row represents a single trial and each column represents the probability for one class (i.e., one of the four RDKs and blank ITI). The probabilities in each row sum to 1, reflecting the relative likelihoods across all classes for that trial. The highest probability determines the decoded label when computing decoding accuracy. Finally, averaging these probabilities across trials yields five values that indicate the overall likelihood of the predicted stimulus belonging to a given class.

Optimal time point of motion direction representation

The optimal time point of motion direction representation was considered as the time point with the highest decoding accuracy in the functional localizer data. To index the optimal time point of each motion direction for each participant, we conducted a time-resolved motion direction decoding analysis on the functional localizer data using Lasso-regularized logistic regression models. A leave-one-trial-out cross-validation procedure was used to train the classifier to determine one of the four motion directions, yielding a decoding accuracy at each time point for

each participant. Finally, the time point with the highest decoding accuracy was independently extracted for each participant and each motion direction. These time points are referred to as optimal time points and were used for training feature-specific decoding models.

Sequenceness measure

To identify sequenceness during the post-cue blank period in each trial, we trained models to detect transient spontaneous neural reactivation of each motion direction representation. Therefore, a one-versus-rest Lasso-regularized logistic regression model was trained separately for each participant and motion direction using the functional localizer data. MEG signals from the 72 occipital sensors obtained throughout all localizer scanning sessions were used to train the decoding models. As our aim was to quantify the evidence of feature-specific sequence, for each motion direction, we trained a binomial classifier, using positive instances from trials in which that feature (e.g., 0°) was presented and negative instances from trials in which all other features (e.g., 90°, 180°, and 270°) were presented, together with an equivalent amount of null data from the 1–1.5 s ITI. The sensor distributions of beta estimates and the spatial correlation among the classifiers are shown in **Figure S1**.

The analysis pipeline of sequenceness is illustrated in **Figure 3**. We first applied the trained models to MEG signals at each time point during the blank period, to generate a [time x motion direction] reactivation probability (i.e., decoding probability) matrix for each trial (**Figure S2**). The TDLM framework was then used to quantify evidence for sequential reactivations consistent with the exposed motion sequence (Liu et al., 2021b, 2021a; Nour et al., 2021).

TDLM is a multiple linear regression approach to quantify the extent to which a lagged reactivation time course of one motion direction i, $(X(\Delta t)_i$, Δt indicates lag time) can predict the reactivation time course of another motion direction j, (X_j). Two steps were included in this pipeline. First, we performed multiple separate regressions using the reactivation time course of each motion direction as a dependent variable (j ∈ [1: 4]) and the historical (i.e., time-lagged) reactivation time courses of all motion directions (i ∈ [1: 4]) as predictor variables.

$$X_j = \sum_{i=1}^{4} X(\Delta t)_i * \beta(\Delta t)_{i,j} + C \qquad (1)$$

The predictor $X(\Delta t)_i$ was a Δt-lagged copy of the reactivation time course of X_i. The regression coefficients $\beta(\Delta t)_{i,j}$ quantify the evidence for each empirical motion direction → motion direction reactivation pattern at a given time lag, Δt. For example, if X_j represents the reactivation time course of 0° during the blank period in the main phase, and X_i represents the reactivation time course of 90° during the same period, then $\beta(\Delta t)_{i,j}$ is the coefficient that captures the unique variance in the reactivation time course of 0° explained by the Δt-lagged reactivation time course of 90° (**Figure 3D**, 1st level GLM analysis). Finally, all such first-level coefficients were placed in a lag-specific [4 x 4] empirical transition matrix ***B***, representing evidence for all possible transitions at a specific lag.

In the second step, we quantified evidence supporting that the empirical (lag-specific) transition matrix, ***B***, can be predicted by the sequences of interest, i.e., the exposed motion sequence. All transitions of interest were specified in a model transition matrix (**Figure 3D**, 2nd level GLM analysis; 1 for transitions of interest and 0 otherwise), separately for forward (as in the motion sequence) (T_F), and backward (opposite to the motion sequence) direction (T_B). Then, the strength of all sequences of interest was measured by:

$$\boldsymbol{B} = \sum_{r=1}^{4} Z_r * T_r \qquad (2)$$

where $\boldsymbol{B}$ is the [4 x 4] empirical (lag-specific) transition matrix that acquired from the data, T_r is the [4 x 4] predictor transition matrix (for regressor r), and Z_r is the scalar regression coefficient quantifying the evidence that the hypothesized transitions T_r predict the empirical transitions, $\boldsymbol{B}$. We included four predictor matrices: (1) T_F: transitions as in the motion sequence in the forward direction (transitions corresponding to [0° → 90° → 180° → 270°]), (2) T_B: transitions opposite to the motion sequence in the backward direction ([270° → 180° → 90° → 0°], T_B is the transpose of T_F), (3) T_{auto}: self-transitions to control for autocorrelation ([4 x 4] identity matrix), and (4) T_{const}: a constant matrix to model away the average of all transitions, ensuring that any weight on T_F and T_B was not due to general background neural dynamics.

Notably, the estimate of sequence strength, Z_r, is a relative quantity. An estimate of zero for 0° to 90°, for example, does not mean lack of replay from 0° → 90° but no stronger replay of 0° → 90° than that of other transitions. Repeating the regression in **Equation 2** at each time lag (Δt = 4, 8, 12, …, 600 ms) results in both forward and backward sequence strength as a function of time lag. Shorter lags indicate greater time compression, corresponding to faster speeds.

In the current study, sequenceness was defined based on the contrast between the evidence for the motion sequence replay in the forward ([0° → 90° → 180° → 270°]) versus backward ([270° → 180° → 90° → 0°]) direction (i.e., $Z_1 - Z_2$); thus, removing between-participant variance in the sequential replay per se (Liu et al., 2021a; Nour et al., 2021). Positive sequenceness values indicate replay in a predominantly forward direction, whereas negative sequenceness values indicate replay in a predominantly backward direction.

For statistical inference, we used nonparametric permutation tests involving all possible permutations of the stimulus labels at the second-level regression, equivalent to permuting the rows and columns together of the transition matrices used to calculate sequenceness. For each permutation, we calculated the peak absolute mean sequence strength over participants and across lags (controlling for multiple comparisons across lags). Sequence strength in unpermuted data was considered significant if its absolute magnitude was >95% of the within-permutation peak.

Identifying replay onsets and analyzing time-frequency

Having identified that the replay transition at the group level was a 32 ms-lag, we next identified replay onsets. Replay onset was defined as the time point when a strong reactivation of one motion direction (e.g., 0°) was followed by a strong reactivation of the next motion direction (e.g., 90°) in the sequence, with a 32 ms-lag (Liu et al., 2019; Nour et al., 2021). We first generated a matrix Orig as

$$Orig = X * T \quad (3)$$

where X is the [time x motion direction] reactivation matrix, and T is the backward transition matrix. The transition matrix T defines the mapping between the motion direction corresponding to column i in X, and column i in Orig. For example, column 1 in X is the reactivation time course of the motion direction 0°, while column 1 in Orig is the reactivation time course of the motion direction 90°. We then shifted each column of X by Δt = 32 ms, to generate another matrix Proj,

$$Proj = X(\Delta t) \quad (4)$$

where row i in Proj corresponds to row i + 32 ms in X. Next, we multiplied Proj and Orig elementwise, summing over the columns of the resulting matrix; therefore, creating a [time x 1] vector, R, in which each element (i.e., row) indicates the strength of replay with a 32 ms-lag at a given time.

$$R_t = \sum_{i=1}^{4} Orig_{ti} * Proj_{ti} \quad (5)$$

Finally, we identified putative replay event onsets by thresholding R at its 95th percentile preceded by a 100 ms pre-onset baseline exhibiting a low probability of replay at each time point.

We then epoched MEG data in the blank period surrounding each onset and computed a frequency decomposition (wavelet transformation) in the time window of −100–150 ms using all sensors. We aimed to find evidence for the power increase in the high-frequency (120–160 Hz) region of interest at replay onset, compared with a pre-onset baseline (−100–−50 ms from onset), similar to a previous study (Liu et al., 2019). Finally, we generated two separate [time x frequency] matrices (i.e., using forward and backward transition matrices separately) by averaging estimates over sensors and events, capturing the typical spectrum-resolved power change at replay onset.

MEG source reconstruction

We identified the neural sources associated with increased ripple power at putative replay onsets. Forward models were generated based on a single shell using the superposition of basic functions that approximately correspond to the plane tangential to the MEG sensor array. Linearly constrained minimum variance beamforming (Van Veen et al., 1997) was used to reconstruct the epoched MEG data to a grid in MNI space (grid step, 5 mm). The sensor covariance matrix for beamforming was estimated using broadband power data across all frequencies. The baseline activity was the mean activity averaged over −100–−50 ms relative to replay onset. All nonartifactual replay epochs were baseline-corrected at source level. We obtained whole-brain results for voxels predicted by participant-specific ripple power at replay onset. Nonparametric permutation tests were performed on the volume of interest to compute the multiple comparison p values of clusters >10 voxels (whole-brain corrected, cluster-defining threshold; t = 3.1, n = 5000 permutations).

Supplementary information

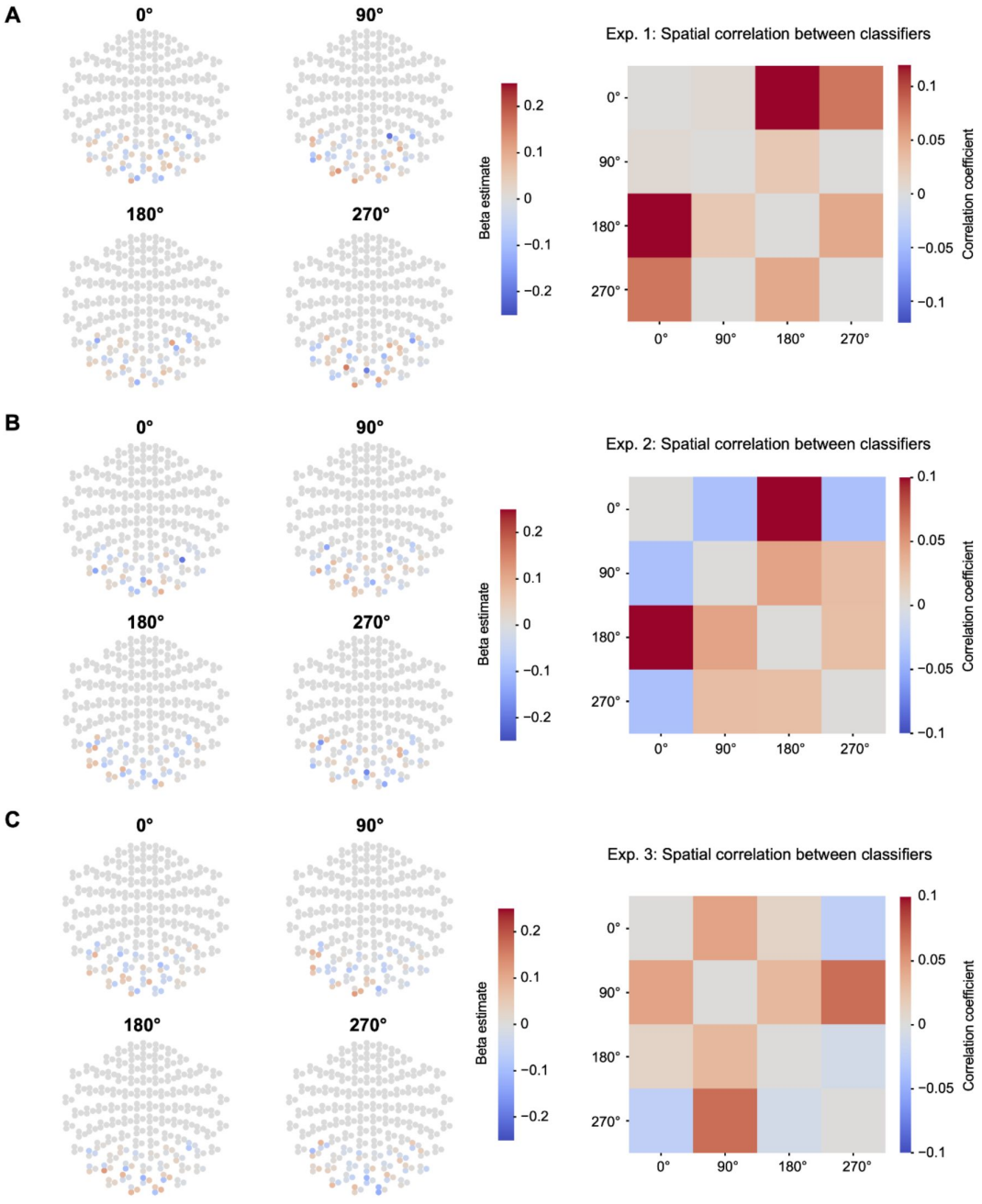

Figure S1.

Sensor maps and spatial correlation of trained Lasso logistic regression models (related to Figure 3)

(A) Left: Sensor map for each state decoding model in Experiment 1; MEG signals from 72 occipital sensors were selected as features while training the classifier. Right: Correlation matrix among classifiers. No spatial correlation was found among trained classifiers (highest correlation; $r < 0.12$). **(B and C)** Same as (A), except the sensor maps and correlation matrix correspond to Experiments 2 (Panel B, highest correlation; $r < 0.1$) and 3 (Panel C, highest correlation; $r < 0.1$), respectively.

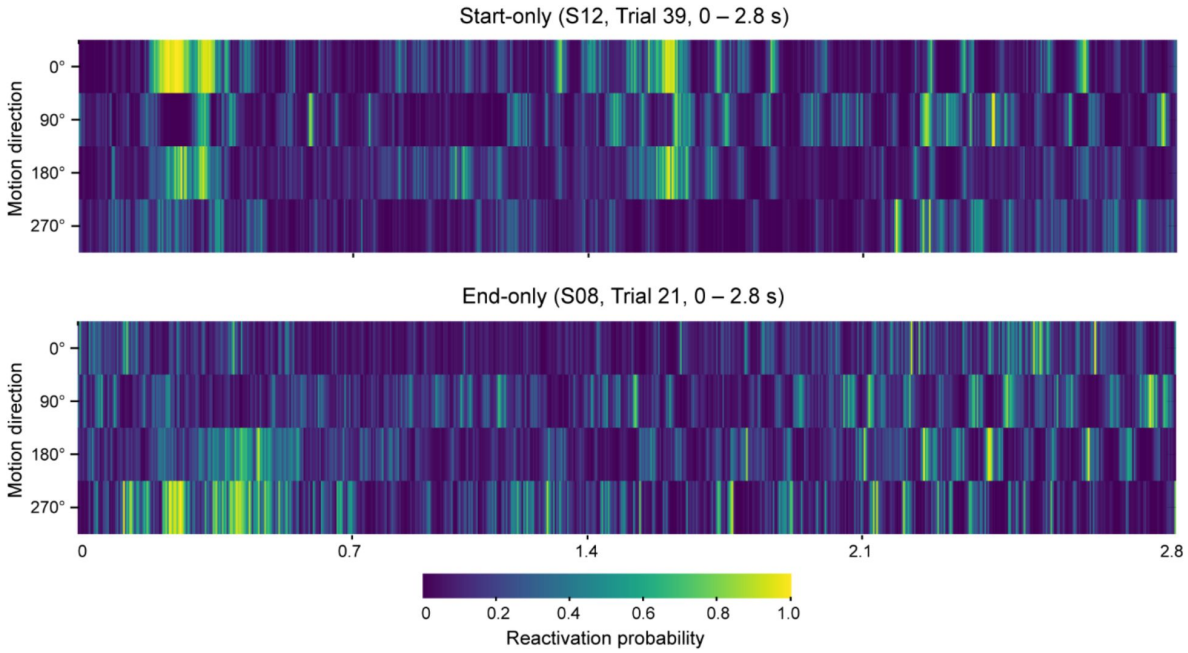

Figure S2.

Decoded feature representations in start- and end-only conditions (related to Figures 3)

Time series of reactivation probability output from the four regression models on an example trial. Time zero corresponds to trial onset. Both participants S08 and S12 were exposed with a fixed motion sequence of 0° → 90° → 180° → 270°.

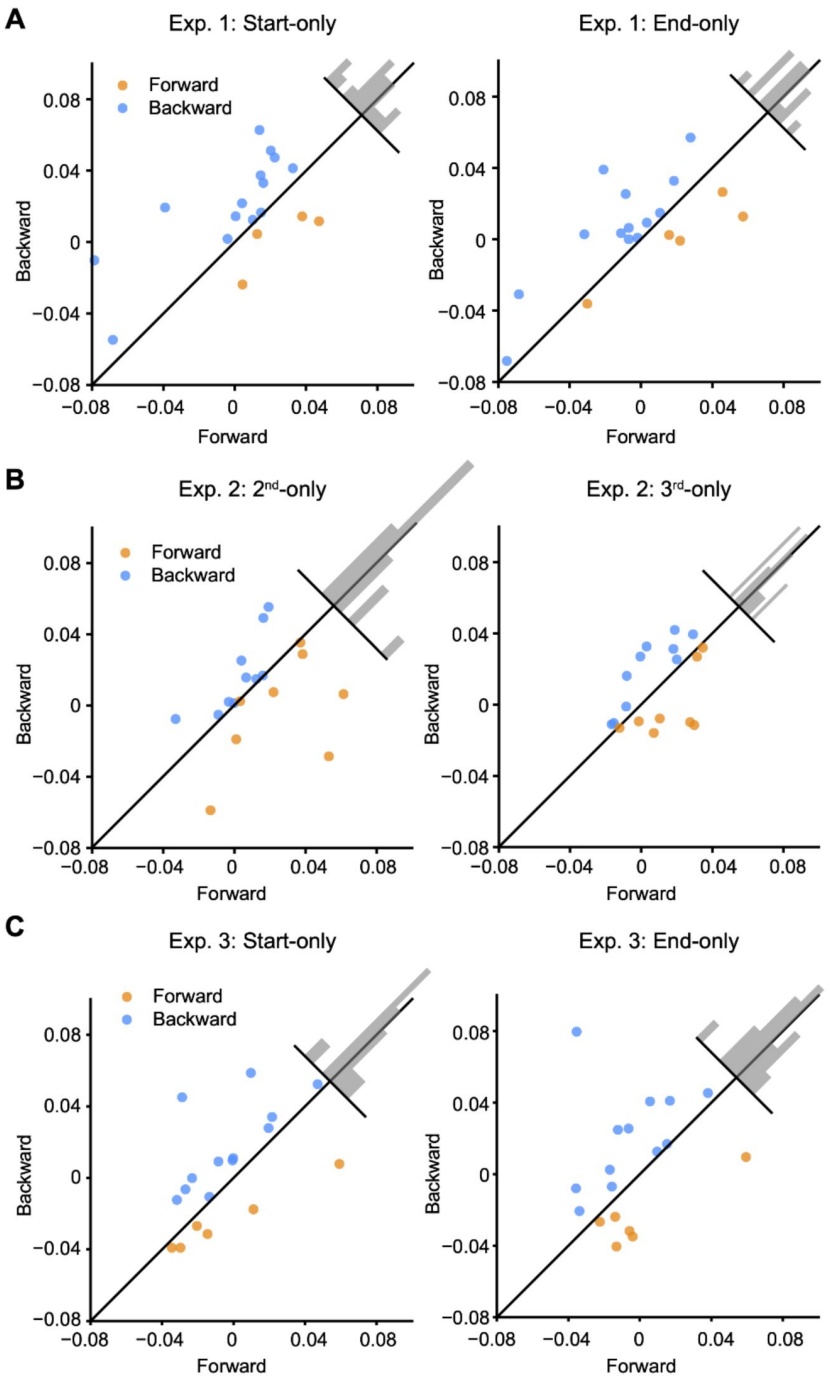

Figure S3.

Sequenceness distribution across participants (related to Figures 4 and 5)

(A) In Experiment 1, of the 18 participants, 14 showed backward replay at 32 ms-lag for the start-only condition (left), and 13 showed backward replay at 32 ms-lag for the end-only condition (right). Each dot represents an individual participant. Backward and forward sequenceness is denoted by blue and yellow dots, respectively. The inset histogram shows the distribution of deviations from the unity line. **(B)** Same as described in (A), but for the results of Experiment 2 in the 2nd-only (left) and 3rd-only (right) conditions, respectively. **(C)** Same as described in (A) but for the results of Experiment 3 in the start- (left) and end-only (right) conditions, respectively.

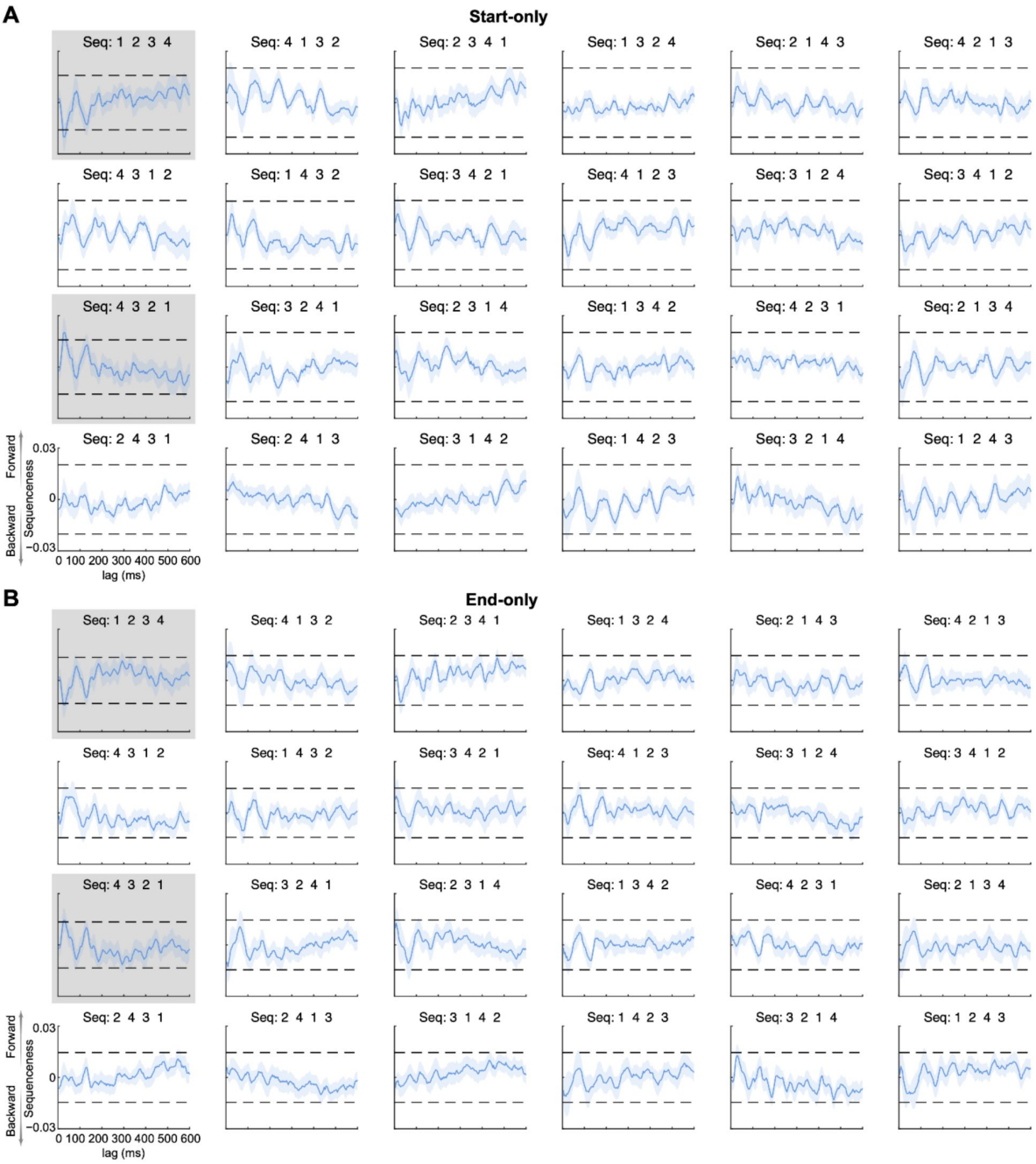

Figure S4.

Sequenceness for each of the 24 possible orders (related to Figure 4)

(A) In the start-only condition of Experiment 1, only the backward sequence [4 → 3 → 2 → 1] with lags at 28–40 ms was significantly different (gray panels). The horizontal dashed lines represent significance thresholds derived from state label permutation at the 2nd-level GLM matrix of temporally delayed linear modeling. **(B)** Same as described in (A) but for the end-only condition in Experiment 1.

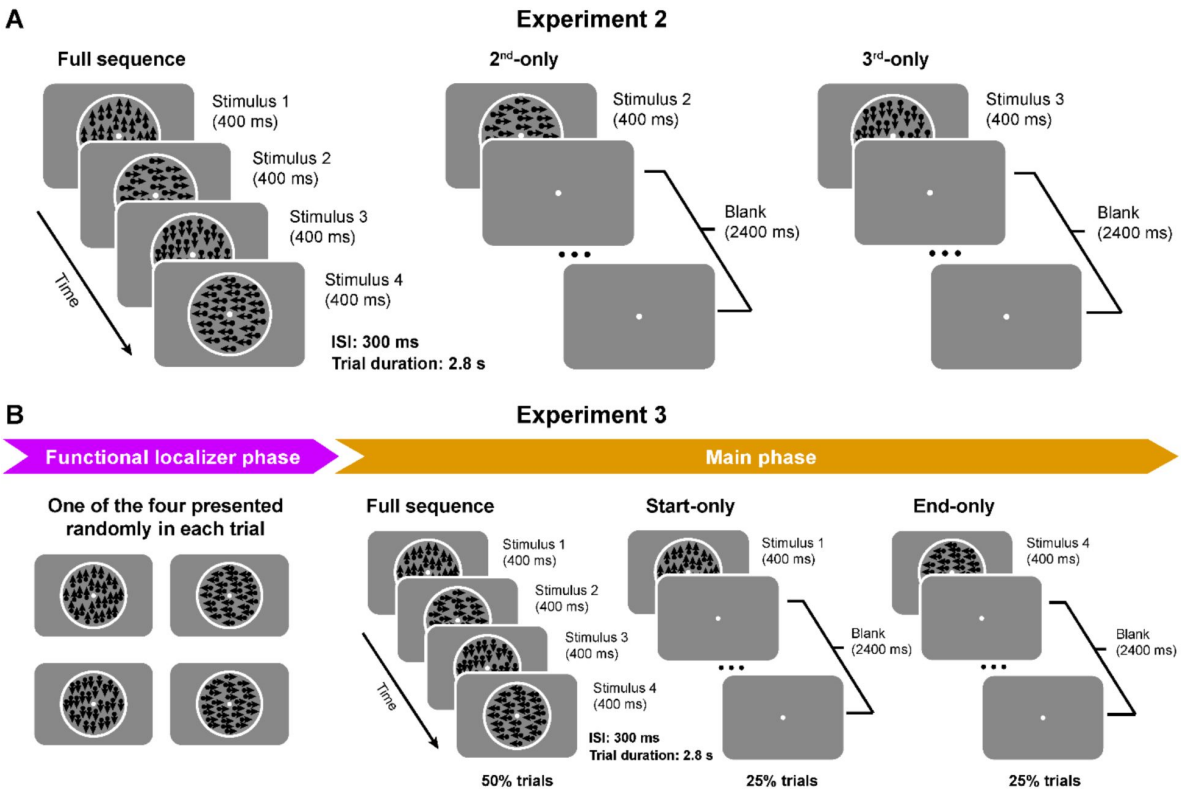

Figure S5.

Stimuli and experimental procedures in Experiments 2 and 3 (related to Figure 5)

(A) We presented the second (2nd-only condition) or third RDK (3rd-only condition) as a cue in Experiment 2. **(B)** The procedure of Experiment 3 was identical to that of Experiment 1 except for removing the exposure phase.

Data and Code availability

Data used to generate the findings of this study will be available upon request (subject to participant consent) to the Lead Contact. TDLM MATLAB Code available at: *https://github.com/YunzheLiu/TDLM*. Custom computer code will be made available upon request to the Lead Contact.

Acknowledgements

This study was supported by National Science and Technology Innovation 2030 Major Program (2022ZD0204802), the National Natural Science Foundation of China (T2421004, 31930053, 32400874), Beijing Natural Science Foundation (5244044), and the Young Scientists Fund of the Humanities and Social Science Foundation of Ministry of Education of China (23YJCZH071).

Additional information

Author contributions

Conceptualization, T.H., Y.L., and F.F.; Investigation, T.H., Q.W., X.G., and X.Z.; Writing – Original Draft, T.H.; Writing – Review & Editing, T.H., Q.W., X.Z., Y.L., and F.F.

References

Alvarez P, Squire LR (1994) **Memory consolidation and the medial temporal lobe: a simple network model** *Proc Natl Acad Sci U S A* **91**:7041–7045

Ambrose RE, Pfeiffer BE, Foster DJ (2016) **Reverse Replay of Hippocampal Place Cells Is Uniquely Modulated by Changing Reward** *Neuron* **91**:1124–1136

Auksztulewicz R, Myers NE, Schnupp JW, Nobre AC (2019) **Rhythmic Temporal Expectation Boosts Neural Activity by Increasing Neural Gain** *J Neurosci* **39**:9806–9817

Baker R, Dexter M, Hardwicke TE, Goldstone A, Kourtzi Z (2014) **Learning to predict: Exposure to temporal sequences facilitates prediction of future events** *Vision Res* **99**:124–133

Barne LC, Cravo AM, de Lange FP, Spaak E (2022) **Temporal prediction elicits rhythmic preactivation of relevant sensory cortices** *European Journal of Neuroscience* **55**:3324–3339

Buch ER, Claudino L, Quentin R, Bönstrup M, Cohen LG (2021) **Consolidation of human skill linked to waking hippocampo-neocortical replay** *Cell Rep* **35**:109193

Buonomano DV, Merzenich MM (1998) **CORTICAL PLASTICITY: From Synapses to Maps** *Annual Review of Neuroscience* **21**:149–186

Bush D, Ólafsdóttir HF, Barry C, Burgess N (2022) **Ripple band phase precession of place cell firing during replay** *Current Biology* **32**:64–73

Buzsáki G (1986) **Hippocampal sharp waves: Their origin and significance** *Brain Research* **398**:242–252

Buzsáki G (1996) **The hippocampo-neocortical dialogue** *Cereb Cortex* **6**:81–92

Buzsáki G (2015) **Hippocampal sharp wave-ripple: A cognitive biomarker for episodic memory and planning** *Hippocampus* **25**:1073–1188

Carr MF, Jadhav SP, Frank LM (2011) **Hippocampal replay in the awake state: a potential substrate for memory consolidation and retrieval** *Nat Neurosci* **14**:147–153

Chen N, Cai P, Zhou T, Thompson B, Fang F (2016) **Perceptual learning modifies the functional specializations of visual cortical areas** *Proceedings of the National Academy of Sciences* **113**:5724–5729

Chun MM, Phelps EA (1999) **Memory deficits for implicit contextual information in amnesic subjects with hippocampal damage** *Nat Neurosci* **2**:844–847

Costandi M (2016) **Neuroplasticity** MIT Press

Demarchi G, Sanchez G, Weisz N (2019) **Automatic and feature-specific prediction-related neural activity in the human auditory system** *Nat Commun* **10**:3440

Diba K, Buzsáki G (2007) **Forward and reverse hippocampal place-cell sequences during ripples** *Nat Neurosci* **10**:1241–1242

Dimakopoulos V, Mégevand P, Stieglitz LH, Imbach L, Sarnthein J (2022) **Information flows from hippocampus to auditory cortex during replay of verbal working memory items** *eLife* **11**:e78677

Eagleman SL, Dragoi V (2012) **Image sequence reactivation in awake V4 networks** *PNAS* **109**:19450–19455

Eichenbaum H, Yonelinas AR, Ranganath C (2007) **The Medial Temporal Lobe and Recognition Memory** *Annu Rev Neurosci* **30**:123–152

Ekman M, Kok P, de Lange FP (2017) **Time-compressed preplay of anticipated events in human primary visual cortex** *Nat Commun* **8**:15276

Ekman M, Kusch S, de Lange FP (2023) **Successor-like representation guides the prediction of future events in human visual cortex and hippocampus** *eLife* **12**:e78904

Fang F, Murray SO, Kersten D, He S (2005) **Orientation-Tuned fMRI Adaptation in Human Visual Cortex** *Journal of Neurophysiology* **94**:4188–4195

Finnie PSB, Komorowski RW, Bear MF (2021) **The spatiotemporal organization of experience dictates hippocampal involvement in primary visual cortical plasticity** *Current Biology* **31**:3996–4008

Foster DJ, Wilson MA (2006) **Reverse replay of behavioural sequences in hippocampal place cells during the awake state** *Nature* **440**:680

Garvert MM, Dolan RJ, Behrens TE (2017) **A map of abstract relational knowledge in the human hippocampal–entorhinal cortex** *eLife* **6**:e17086

Gavornik JP, Bear MF (2014) **Learned spatiotemporal sequence recognition and prediction in primary visual cortex** *Nat Neurosci* **17**:732–737

Gillespie AK, Maya DAA, Denovellis EL, Liu DF, Kastner DB, Coulter ME, Roumis DK, Eden UT, Frank LM (2021) **Hippocampal replay reflects specific past experiences rather than a plan for subsequent choice** *Neuron* **109**:3149–3163

Gothard KM, Skaggs WE, Moore KM, McNaughton BL (1996) **Binding of hippocampal CA1 neural activity to multiple reference frames in a landmark-based navigation task** *J Neurosci* **16**:823–835

Gridchyn I, Schoenenberger P, O'Neill J, Csicsvari J (2020) **Assembly-Specific Disruption of Hippocampal Replay Leads to Selective Memory Deficit** *Neuron* **106**:291–300

Gutnisky DA, Hansen BJ, Iliescu BF, Dragoi V (2009) **Attention Alters Visual Plasticity during Exposure-Based Learning** *Current Biology* **19**:555–560

Hannula DE, Tranel D, Cohen NJ (2006) **The Long and the Short of It: Relational Memory Impairments in Amnesia, Even at Short Lags** *J Neurosci* **26**:8352–8359

Henke K (2010) **A model for memory systems based on processing modes rather than consciousness** *Nat Rev Neurosci* **11**:523–532

Herrmann B, Henry MJ, Haegens S, Obleser J (2016) **Temporal expectations and neural amplitude fluctuations in auditory cortex interactively influence perception** *NeuroImage* **124**:487–497

Hindy NC, Ng FY, Turk-Browne NB (2016) **Linking pattern completion in the hippocampus to predictive coding in visual cortex** *Nat Neurosci* **19**:665–667

Hsieh L-T, Gruber MJ, Jenkins LJ, Ranganath C (2014) **Hippocampal Activity Patterns Carry Information about Objects in Temporal Context** *Neuron* **81**:1165–1178

Igata H, Ikegaya Y, Sasaki T (2021) **Prioritized experience replays on a hippocampal predictive map for learning** *Proceedings of the National Academy of Sciences* **118**:e2011266118

Ji D, Wilson MA (2007) **Coordinated memory replay in the visual cortex and hippocampus during sleep** *Nature Neuroscience* **10**:100–107

Joo HR, Frank LM (2018) **The hippocampal sharp wave–ripple in memory retrieval for immediate use and consolidation** *Nat Rev Neurosci* **19**:744–757

Kok P, Failing M, de Lange F (2014) **Prior Expectations Evoke Stimulus Templates in the Primary Visual Cortex** *Journal of cognitive neuroscience* **26**

Kok P, Jehee JFM, de Lange FP (2012) **Less Is More: Expectation Sharpens Representations in the Primary Visual Cortex** *Neuron* **75**:265–270

Kok P, Mostert P, Lange FP de (2017) **Prior expectations induce prestimulus sensory templates** *PNAS* **114**:10473–10478

Kok P, Turk-Browne NB (2018) **Associative Prediction of Visual Shape in the Hippocampus** *J Neurosci* **38**:6888–6899

Konkel A, Warren D, Duff M, Tranel D, Cohen N (2008) **Hippocampal amnesia impairs all manner of relational memory** *Frontiers in Human Neuroscience* **2**

Kurth-Nelson Z, Economides M, Dolan RJ, Dayan P (2016) **Fast Sequences of Non-spatial State Representations in Humans** *Neuron* **91**:194–204

Lakatos P, Karmos G, Mehta AD, Ulbert I, Schroeder CE (2008) **Entrainment of Neuronal Oscillations as a Mechanism of Attentional Selection** *Science* **320**:110–113

Lakatos P, Musacchia G, O'Connel MN, Falchier AY, Javitt DC, Schroeder CE (2013) **The Spectrotemporal Filter Mechanism of Auditory Selective Attention** *Neuron* **77**:750–761

Lee AK, Wilson MA (2002) **Memory of Sequential Experience in the Hippocampus during Slow Wave Sleep** *Neuron* **36**:1183–1194

Li W (2016) **Perceptual Learning: Use-Dependent Cortical Plasticity** *Annual Review of Vision Science* **2**:109–130

Liu Y, Dolan RJ, Higgins C, Penagos H, Woolrich MW, Ólafsdóttir HF, Barry C, Kurth-Nelson Z, Behrens TE (2021a) **Temporally delayed linear modelling (TDLM) measures replay in both animals and humans** *eLife* **10**:e66917

Liu Y, Dolan RJ, Kurth-Nelson Z, Behrens TEJ (2019) **Human Replay Spontaneously Reorganizes Experience** *Cell* **178**:640–652

Liu Y, Mattar MG, Behrens TEJ, Daw ND, Dolan RJ (2021b) **Experience replay is associated with efficient nonlocal learning** *Science* **372**

Liu Y, Nour MM, Schuck NW, Behrens TEJ, Dolan RJ (2022) **Decoding cognition from spontaneous neural activity** *Nat Rev Neurosci* :1–11

Lu J, Luo L, Wang Q, Fang F, Chen N (2020) **Cue-triggered activity replay in human early visual cortex** *Sci China Life Sci*

Lu Z-L, Dosher BA (2022) **Current directions in visual perceptual learning** *Nat Rev Psychol* **1**:654–668

Marr D, Brindley GS (1971) **Simple memory: a theory for archicortex** *Philos Trans R Soc Lond B Biol Sci* **262**:23–81

McFadyen J, Liu Y, Dolan RJ (2023) **Differential replay of reward and punishment paths predicts approach and avoidance** *Nat Neurosci* **26**:627–637

Mo C, Lu J, Wu B, Jia J, Luo H, Fang F (2019) **Competing rhythmic neural representations of orientations during concurrent attention to multiple orientation features** *Nat Commun* **10**:1–10

Nour MM, Liu Y, Arumuham A, Kurth-Nelson Z, Dolan RJ (2021) **Impaired neural replay of inferred relationships in schizophrenia** *Cell* **184**:4315–4328

O'Keefe J, Nadel L (1978) **The hippocampus as a cognitive map** Oxford : New York: Clarendon Press

Ólafsdóttir HF, Barry C, Saleem AB, Hassabis D, Spiers HJ (2015) **Hippocampal place cells construct reward related sequences through unexplored space** *eLife* **4**:e06063

Ólafsdóttir HF, Carpenter F, Barry C (2016) **Coordinated grid and place cell replay during rest** *Nat Neurosci* **19**:792–794

Ólafsdóttir HF, Carpenter F, Barry C (2017) **Task Demands Predict a Dynamic Switch in the Content of Awake Hippocampal Replay** *Neuron* **96**:925–935

Pojoga SA, Kharas N, Dragoi V (2020) **Perceptually unidentifiable stimuli influence cortical processing and behavioral performance** *Nat Commun* **11**:6109

Redish AD, Rosenzweig ES, Bohanick JD, McNaughton BL, Barnes CA (2000) **Dynamics of Hippocampal Ensemble Activity Realignment: Time versus Space** *J Neurosci* **20**:9298–9309

Redish AD, Touretzky DS (1998) **The role of the hippocampus in solving the Morris water maze** *Neural Comput* **10**:73–111

Rivard B, Li Y, Lenck-Santini P-P, Poucet B, Muller RU (2004) **Representation of objects in space by two classes of hippocampal pyramidal cells** *J Gen Physiol* **124**:9–25

Roelfsema PR, de Lange FP (2016) **Early Visual Cortex as a Multiscale Cognitive Blackboard** *Annual Review of Vision Science* **2**:131–151

Rolls ET (2000) **Hippocampo-cortical and cortico-cortical backprojections** *Hippocampus* **10**:380–388

Sasaki Y, Nanez JE, Watanabe T (2010) **Advances in visual perceptual learning and plasticity** *Nat Rev Neurosci* **11**:53–60

Schapiro AC, Gregory E, Landau B, McCloskey M, Turk-Browne NB (2014) **The necessity of the medial temporal lobe for statistical learning** *J Cogn Neurosci* **26**:1736–1747

Staresina BP, Davachi L (2009) **Mind the Gap: Binding Experiences across Space and Time in the Human Hippocampus** *Neuron* **63**:267–276

Taulu S, Simola J (2006) **Spatiotemporal signal space separation method for rejecting nearby interference in MEG measurements** *Phys Med Biol* **51**:1759–1768

Turk-Browne NB, Scholl BJ, Chun MM, Johnson MK (2009) **Neural evidence of statistical learning: efficient detection of visual regularities without awareness** *J Cogn Neurosci* **21**:1934–1945

Turner W, Blom T, Hogendoorn H (2023) **Visual Information Is Predictively Encoded in Occipital Alpha/Low-Beta Oscillations** *J Neurosci* **43**:5537–5545

Van Veen BD, van Drongelen W, Yuchtman M, Suzuki A (1997) **Localization of brain electrical activity via linearly constrained minimum variance spatial filtering** *IEEE Trans Biomed Eng* **44**:867–880

Watanabe T, Sasaki Y (2015) **Perceptual learning: Toward a comprehensive theory** *Annu Rev Psychol* **66**:197–221

Whittington JCR, Muller TH, Mark S, Chen G, Barry C, Burgess N, Behrens TEJ (2020) **The Tolman-Eichenbaum Machine: Unifying Space and Relational Memory through Generalization in the Hippocampal Formation** *Cell* **183**:1249–1263

Wimmer GE, Liu Y, Vehar N, Behrens TEJ, Dolan RJ (2020) **Episodic memory retrieval success is associated with rapid replay of episode content** *Nature Neuroscience* **23**:1025–1033

Wyart V, Nobre AC, Summerfield C (2012) **Dissociable prior influences of signal probability and relevance on visual contrast sensitivity** *PNAS* **109**:3593–3598

Xu S, Jiang W, Poo M, Dan Y (2012) **Activity recall in a visual cortical ensemble** *Nature Neuroscience* **15**:449–455

Author information

Tao He

Center for the Cognitive Science of Language, Beijing Language and Culture University, Beijing, China, Key Laboratory of Language Cognitive Science (Ministry of Education), Beijing Language and Culture University, Beijing, China, School of Psychological and Cognitive Sciences and Beijing Key Laboratory of Behavior and Mental Health, Peking University, Beijing, China, IDG/McGovern Institute for Brain Research, Peking University, Beijing, China
ORCID iD: 0000-0002-1009-0500

Xizi Gong
School of Psychological and Cognitive Sciences and Beijing Key Laboratory of Behavior and Mental Health, Peking University, Beijing, China, IDG/McGovern Institute for Brain Research, Peking University, Beijing, China

Qian Wang
School of Psychological and Cognitive Sciences and Beijing Key Laboratory of Behavior and Mental Health, Peking University, Beijing, China, IDG/McGovern Institute for Brain Research, Peking University, Beijing, China

Xinyi Zhu
School of Psychological and Cognitive Sciences and Beijing Key Laboratory of Behavior and Mental Health, Peking University, Beijing, China, IDG/McGovern Institute for Brain Research, Peking University, Beijing, China

Yunzhe Liu
Chinese Institute for Brain Research, Beijing, China

Fang Fang
School of Psychological and Cognitive Sciences and Beijing Key Laboratory of Behavior and Mental Health, Peking University, Beijing, China, IDG/McGovern Institute for Brain Research, Peking University, Beijing, China, Peking-Tsinghua Center for Life Sciences, Peking University, Beijing, China, Key Laboratory of Machine Perception (Ministry of Education), Peking University, Beijing, China
ORCID iD: 0000-0002-7718-2354

For correspondence: ffang@pku.edu.cn

Editors

Reviewing Editor
Peter Kok
University College London, London, United Kingdom

Senior Editor
Laura Colgin
University of Texas at Austin, Austin, United States of America

Reviewer #1 (Public review):

Summary:

The study identifies two types of activation: one that is cue-triggered and non-specific to motion directions, and another that is specific to the exposed motion directions but occurs in a reversed manner. The finding that activity in the medial temporal lobe (MTL) preceded that in the visual cortex suggests that the visual cortex may serve as a platform for the manifestation of replay events, which potentially enhance visual sequence learning.

Evaluations:

Identifying the two types of activation after exposure to a sequence of motion directions is very interesting. The experimental design, procedures and analyses are solid. The findings are interesting and novel.

In the original submission, it was not immediately clear to me why the second type of activation was suggested to occur spontaneously. The procedural differences in the analyses that distinguished between the two types of activation need to be a little better clarified. However, this concern has been satisfactorily addressed in the revision.

https://doi.org/10.7554/eLife.101511.2.sa2

Reviewer #2 (Public review):

This paper shows and analyzes an interesting phenomenon. It shows that when people are exposed to sequences of moving dots (That is moving dots in one direction, followed by another direction etc.), that showing either the starting movement direction, or ending movement direction causes a coarse-grained brain response that is similar to that elicited by the complete sequence of 4 directions. However, they show by decoding the sensor responses that this brain activity actually does not carry information about the actual sequence and the motion directions, at least not on the time scale of the initial sequence. They also show a reverse reply on a highly-compressed time scale, which is elicited during the period of elevated activity, and activated by the first and last elements of the sequence, but not others. Additionally, these replays seem to occur during periods of cortical ripples, similar to what is found in animal studies.

These results are intriguing. They are based on MEG recordings in humans, and finding such replays in humans is novel. Also, this is based on what seems to be sophisticated statistical analysis. The statistical methodology seems valid, but due to its complexity it is not easy to understand. The methods especially those described in figures 3 and 4 should be explained better.

https://doi.org/10.7554/eLife.101511.2.sa1

Author response:

The following is the authors' response to the original reviews.

> ***Public Reviews:***
>
> ***Reviewer #1 (Public review):***
>
> *Summary:*
>
> *The study identifies two types of activation: one that is cue-triggered and nonspecific to motion directions, and another that is specific to the exposed motion directions but occurs in a reversed manner. The finding that activity in the medial temporal lobe (MTL) preceded that in the visual cortex suggests that the visual cortex may serve as a platform for the manifestation of replay events, which potentially enhance visual sequence learning.*
>
> *Strengths:*
>
> *Identifying the two types of activation after exposure to a sequence of motion directions is very interesting. The experimental design, procedures, and analyses are solid. The findings are interesting and novel.*
>
> *Weaknesses:*

> *It was not immediately clear to me why the second type of activation was suggested to occur spontaneously. The procedural differences in the analyses that distinguished between the two types of activation need to be a little better clarified.*

We thank the reviewer for his/her summary and constructive feedback on our study. We appreciate the recognition of the strengths of our study.

The second type of activation, namely the replay of feature-specific reactivations, is considered spontaneous because it reflects internally driven neural processes rather than responses directly triggered by external stimuli. Unlike responses evoked by stimuli, spontaneous replay is not time-locked to stimulus onset. Instead, it arises from the brain's intrinsic activity, typically observed during offline periods (e.g., rest or blank period) when external stimuli are absent. This allows the neural system to reactivate and consolidate prior experiences without interference from ongoing external stimuli.

Replay is believed to be a key mechanism underlying various cognitive functions, such as memory consolidation (Gillespie et al., 2021; Gridchyn et al., 2020), learning (Igata et al., 2021), prediction and planning (Ólafsdóttir et al., 2018). Furthermore, the hippocampus and related cortical areas engage in replay to extract abstract relationships from sequential experiences, forming a "template" that can generalize across contexts (Liu et al., 2019). In our study, the feature-specific replay observed during blank periods likely reflects this process, supporting the integration of exposed motion direction sequences into cohesive memory representations and facilitating visual sequence learning.

We have extended the Discussion section to incorporate this explanation (Lines 440 - 447).

Regarding the second question, the procedural differences between the two types of activations lie in the classifiers used for the two analyses: a multiclass classifier for non-specific elevated responses and binary classifiers for feature-specific replay.

For the non-feature-specific elevated responses, we trained a five-class (with the labels of the four RDKs and the ITI (inter-stimulus interval)) classifier on the localizer data and tested on the blank period in the main phase. We attempted to decode motion direction information at each time point at the group level. However, the results revealed no feature-specific information at the group level during the blank period.

For the feature-specific replay, we employed the temporal delayed linear modeling (TDLM) to examine whether individual motion direction information was encoded in a sequential and spontaneous manner. Here, we first needed to train four binary classifiers, each was sensitive to only one motion direction (i.e., 0°, 90°, 180°, or 270°), as our aim was to quantify the evidence of feature-specific sequence in the subsequent analyses. For each classifier, positive instances were trials where the corresponding feature (e.g., 0°) was presented, while negative instances included trials with other features (e.g., 90°, 180°, and 270°) and an equivalent amount of null data from the ITI period (1–1.5 s).

We have clarified these methodological details in the Methods section (Pages 34 – 41).

> ***Reviewer #2 (Public review):***
>
> *This paper shows and analyzes an interesting phenomenon. It shows that when people are exposed to sequences of moving dots (that is moving dots in one direction, followed by another direction, etc.), showing either the starting movement direction or ending movement direction causes a coarse-grained brain response that is similar to that elicited by the complete sequence of 4 directions. However, they show by decoding the sensor responses that this brain activity actually does not carry information about the actual sequence and the motion directions, at least not on the time scale of the initial*

> *sequence. They also show a reverse reply on a highly compressed time scale, which is elicited during the period of elevated activity, and activated by the first and last elements of the sequence, but not others. Additionally, these replays seem to occur during periods of cortical ripples, similar to what is found in animal studies.*
>
> *These results are intriguing. They are based on MEG recordings in humans, and finding such replays in humans is novel. Also, this is based on what seems to be sophisticated statistical analysis. However, this is the main problem with this paper. The statistical analysis is not explained well at all, and therefore its validity is hard to evaluate. I am not at all saying it is incorrect; what I am saying is that given how it is explained, it cannot be evaluated.*

We thank the reviewer's detailed evaluation as well as the acknowledgment of the novelty of our study.

To address the concern about the statistical analysis, in the revised manuscript, we have modified the Methods section to provide a more detailed explanation of the analytical pipeline, particularly for several important aspects such as decoding probability and TDLM. (Lines 646 – 657, Lines 682 – 734).

Below, we provide point-by-point responses to further elaborate on these revisions and address the reviewer's comments.

> ***Recommendations for the authors:***
>
> ***Reviewer #1 (Recommendations for the authors):***
>
> *I have questions.*
>
> *(1) Participants were exposed to a predefined sequence of motion directions either clockwise or counterclockwise. Is it possible that the observed replay is related to the activation of MST neurons? If a predetermined sequence is not in either clockwise or counterclockwise but is randomly determined like 0{degree sign}->180{degree sign}->270{degree sign}->90{degree sign}, would the same result be obtained?*

We thank the reviewer for these thoughtful questions.

First, regarding the potential involvement of MST neurons, it is plausible that the observed replay might involve activity in motion-sensitive brain regions, including the medial superior temporal (MST) and even middle temporal (MT) areas. MST neurons, located in the extrastriate visual cortex, are highly direction-selective and are known for their sensitivity to complex motion patterns, such as rotations and expansions (Duffy & Wurtz, 1991; Saito et al., 1986). In our experiment, the use of RDKs with four distinct motion directions might elicit responses in MST neurons. However, due to the limited spatial resolution of MEG, we cannot provide direct evidence for this claim.

Second, regarding the impact of randomly ordered sequences, we believe that the replay patterns would still occur even if the sequences were randomly ordered (e.g., 0° → 180° → 270° → 90°). After a sequence is repeatedly exposed, the hippocampus has the capacity to encode abstract relationships in the sequence. Evidence supporting this view comes from previous studies. For example, Liu et al., (2019) showed that replay does not merely recapitulate visual experience but can also follow a sequence implied by learned abstract knowledge. In their study, participants were instructed that viewing pictures C→D, B→C, and A→B implies a true sequence of A→B→C→D. During subsequent testing, they observed replay events following this learned true sequence, even with novel visual stimuli, indicating that the brain maintains sequence knowledge independent of specific stimuli. Similarly, Ekman et al., (2023) showed that prediction-based neural responses could be observed when moving

dots were presented in a random order rather than in a clockwise or counterclockwise order, which correspond to the four motion directions in our study.

Together, these studies suggest that replay mechanisms in the brain are flexible and can encode and reproduce abstract relationships between sequential stimuli, regardless of their specific spatial contents. Therefore, we believe that even if the sequence were randomly ordered, the same backward replay pattern would still be observed.

> *(2) Is it possible that the motion direction non-specific responses actually reflect the replay of another feature of the exposed sequence, namely, the temporally rhythmic presentations of the sequence, rather than suggested in the discussion?*

We thank the reviewer for raising this insightful possibility.

There is substantial evidence that rhythmic stimulation can entrain neural oscillations, which in turn facilitates predictions about future inputs and enhances the brain's readiness for incoming stimuli (Barne et al., 2022; Herrmann et al., 2016; Lakatos et al., 2008, 2013). In our study, the temporally rhythmic presentation of the motion sequence may have entrained oscillatory activity in the brain, leading to periodic activation of sensory cortices. This rhythmic entrainment could account for the observed nonspecific responses by reflecting the brain's temporal predictions rather than specific feature replay.

It is important to note that, however, this interpretation is in line with our initial explanation that the non-feature-specific elevated responses likely reflect a general facilitation of neural processes for any upcoming stimuli, rather than being tied to specific stimuli. The rhythmic entrainment mechanism provides another way to understand how the temporal structure in the sequences might contribute to the non-feature-specific elevated responses.

We have revised the Discussion section to incorporate this interpretation, providing a more comprehensive account for the non-feature-specific elevated responses (Lines 428 – 439).

> ***Reviewer #2 (Recommendations for the authors):***
>
> *The main problem with the paper is that the sophisticated statistical methodology is not explained well and therefore its validity is hard to evaluate. I am not at all saying it is incorrect, what I am saying is that given how it is explained, it cannot be evaluated.*

See below for detailed point-by-point responses.

> *The first part is clear. There are 4 directions of motion, and there can also be a blank screen. The random decoding accuracy would be 20%. The decoding methods from the sensors yielded a little above 50% accuracy. This is clearly about chance, but much less than one would get from electrode recording of motion-selective cells in the cortex. However, the concept and methods used here seem clear, in contrast to what comes next.*

Indeed, in the first step, we aimed to validate the reliability of our decoding model by applying a leave-one-out cross validation scheme to the localizer data. Our results showed that the decoding accuracy exceeded 50%, demonstrating robust decoding performance. However, due to the noninvasive nature of MEG and its low spatial resolution, the recorded signals represent population-level activity that inherently includes more noise compared to electrode recordings of motion-selective neurons. Therefore, the decoding accuracy in our study is understandably lower than that obtained with electrode recordings.

> *Next, and most of the paper relies on this concept, they use the term decoding probability (Figure 2). What is the decoding probability measure (Turner 2023)? This is not explained in the methods section. I scanned the Turner et al 2023 paper referenced*

> *and could not find the term decoding probability there. In short, I have no idea what this means. What are these numbers between 0-0.3? How does this relate to accuracies above 50% reported? This is an important concept here, and it is used throughout the paper, so it makes it hard to evaluate the paper.*

We apologize for the lack of clarity in our explanation of the term "decoding probability." Specifically, we used a one-versus-rest Lasso logistic regression model trained on the localizer data to decode the MEG signal patterns elicited by each motion direction during the main phase. The trained model could be used to predict a single label at each time point for each trial (e.g., labels 1 – 4 correspond to the four motion directions and label 5 corresponds to the ITI period). By comparing the predicted label with the true label across test trials, we could compute the time-resolved decoding accuracy as final reports.

Alternatively, rather than predicting a single label for each time point and each trial, the model can also output the probabilities associated with each label/class (e.g., we used the *predict_proba* function in scikit-learn). This results in a 5-column output, where each column represents the probability of the corresponding class, and the sum of the probabilities across the five columns equals 1. Finally, at each time point, averaging these probabilities across trials yields five values that indicate the likelihood of the predicted stimulus belonging to each class.

For example, Figure 2 in the manuscript depicts the decoding probabilities for the four RDKs (the probabilities for the ITI class are not shown in the figure). The number in a cell (between 0 and 0.3) indicates the probability of each class at a given time point (Figure 2A). The decoding probability does not have a direct relationship with the decoding accuracy. However, since there are five classes, the chance level of the decoding probability is 0.2. The highest probability among the five classes at a given time point determines the decoded label when computing the decoding accuracy.

For illustration, in the left panel of Figure 2B, at the onset of the first RDK (0 s), the mean decoding probabilities for the classes 0°, 90°, 180°, 270°, and the blank ITI are 5%, 4.1%, 4.0%, 4.5%, and 82.4%, respectively. Thus, the decoded label should be the blank ITI. In contrast, 0.4 s after the onset of the first RDK, the mean decoding probabilities for the five classes are 28.0%, 19.0%, 22.8%, 21.2%, and 9.0%, respectively. Therefore, the decoded label should be 0°.

We have revised the Methods section to explain this issue (Lines 646 – 657).

> *They did find compressed reversed reply events (Figures 3-4). This is again confusing for several reasons. First, because they use the same unexplained decoding probability measure. Second, the optimal time point defined above depends on the start time of a stimulus, but here the start time is random. Third, the TDLM algorithm is hard to understand. For example, what are the reactivation probabilities of Figure 3C? They do make an effort to explain this in the methods section (lines 652-697) but it's not clear enough from the outset. For example, what does the state X_j is this a vector of activity of sensors? Are these decoding probabilities of the different directions? What is it? Also, what is X_i vs X_i(\Delta t)? Frankly, despite their efforts, I am very confused. Additionally, the figures use the term reactivation probability, where is it defined? So again, the results seem interesting, but the methods are not explained well at all.*
>
> *This paper must better explain the statistical methods so that they can be evaluated. This is not easy, these are relatively complex methods, but they must be explained much better so the validity of the paper can be examined.*

Regarding the optimal time point, we defined it as the time point with the highest decoding accuracy, determined during the validation of the localizer data using a leave-one-out cross-validation scheme. This optimal time point was participant- and motion-direction-specific, as

the latency to achieve the peak decoding accuracy varied across individuals and motion directions. For group-level visualization, we circularly shifted the data over time, aligning each optimal time point to a common reference point (arbitrarily set at 200 ms after stimulus onset). Importantly, however, these time points are unrelated to the data in the main phase, as the models were trained using the independent localizer data and then applied to each time point during the blank period in the main phase.

Regarding the TDLM algorithm, detailed descriptions of the algorithm have been provided in the revised Methods section (Line 683 – 735). Furthermore, we have included explanatory notes in the main text and figure legend to provide immediate context for terms such as "reactivation probability" (Lines 247 – 248, Lines 275 – 276).

> *This paper uses MEG in humans, a non-invasive technique. This allows for such results in humans. Indeed (if the methods are correct) these units can be decoded to provide statistically significant estimates of motion direction. Note, however, that the spatial resolution of MEG is limited. The decoding accuracies of above 50% are way above chance. Note however that if actual motion-sensitive neurons (e.g. area MT) were recorded, and even if the motion is far from 100% coherence, the decoding accuracy would approach 100%.*

We agree with the reviewer that decoding accuracy would approach 100% if single-neuron data from motion-sensitive areas (e.g., area MT) were recorded, given the exceptionally high signal-to-noise ratio (SNR) of such data. However, two considerations inform the methodology of our study.

First, while single-neuron recordings provide invaluable insights, acquiring such data in humans is both ethically challenging and logistically impractical.

Non-invasive MEG, by contrast, offers a practical alternative that can achieve robust decoding of population-level activity with a reasonable SNR.

Second, the primary goal of our study was not merely to achieve high decoding accuracy but also to examine the replay of an exposed motion sequence in the human visual cortex. To achieve this, we first needed to train feature-specific models that can be used to decode the spontaneous reactivations of the four motion directions during the blank period. The ability to distinguish representations of the four motion directions was essential for calculating the “sequenceness” of the exposed motion sequence in the TDLM algorithm. While the absolute decoding accuracy of MEG data may not match that of single-neuron data, an important outcome was the successful construction of feature-specific models for the four motion directions (Figure 3B in the manuscript). These models provided a robust foundation for investigating sequential replay in the brain. These results also align with the broader goal of leveraging MEG data to study dynamic neural processes in humans, even in the face of its spatial resolution limitation.

> *Minor:*
>
> *(1) Line 246 - there is no figure S2A, subplots are not labeled.*

We have corrected this in the revised manuscript.

> *(2) Is Figure 3B referred to in the text? Same for 3C. This figure is there for explaining the statistical models used, but it is not well utilized.*

We have modified the text to clarify this issue in the revised manuscript.

> *(3) English:*

> *There are problems with the use of English in the paper, this should be corrected in the next version. A few examples are below.*
>
> *Noises -> noise*
>
> *- "along the motion path in visual cortex" What does this sentence mean? Is this referring to motion-sensitive areas in the brain? Please clarify.*
>
> *There are many other examples. This is minor, but should be corrected.*

We have corrected these errors in the revised manuscript.

References

Barne, L. C., Cravo, A. M., de Lange, F. P., & Spaak, E. (2022). Temporal prediction elicits rhythmic preactivation of relevant sensory cortices. European Journal of Neuroscience, 55(11–12), 3324–3339. https://doi.org/10.1111/ejn.15405

Ekman, M., Kusch, S., & de Lange, F. P. (2023). Successor-like representation guides the prediction of future events in human visual cortex and hippocampus. eLife, 12, e78904. https://doi.org/10.7554/eLife.78904

Gillespie, A. K., Maya, D. A. A., Denovellis, E. L., Liu, D. F., Kastner, D. B., Coulter, M. E., Roumis, D. K., Eden, U. T., & Frank, L. M. (2021). Hippocampal replay reflects specific past experiences rather than a plan for subsequent choice. Neuron, 109(19), 3149-3163.e6. https://doi.org/10.1016/j.neuron.2021.07.029

Gridchyn, I., Schoenenberger, P., O'Neill, J., & Csicsvari, J. (2020). AssemblySpecific Disruption of Hippocampal Replay Leads to Selective Memory Deficit. Neuron, 106(2), 291-300.e6. https://doi.org/10.1016/j.neuron.2020.01.021

Herrmann, B., Henry, M. J., Haegens, S., & Obleser, J. (2016). Temporal expectations and neural amplitude fluctuations in auditory cortex interactively influence perception. NeuroImage, 124, 487–497. https://doi.org/10.1016/j.neuroimage.2015.09.019

Igata, H., Ikegaya, Y., & Sasaki, T. (2021). Prioritized experience replays on a hippocampal predictive map for learning. Proceedings of the National Academy of Sciences, 118(1), e2011266118. https://doi.org/10.1073/pnas.2011266118

Lakatos, P., Karmos, G., Mehta, A. D., Ulbert, I., & Schroeder, C. E. (2008). Entrainment of Neuronal Oscillations as a Mechanism of Attentional Selection. Science, 320(5872), 110–113. https://doi.org/10.1126/science.1154735

Lakatos, P., Musacchia, G., O'Connel, M. N., Falchier, A. Y., Javitt, D. C., & Schroeder, C. E. (2013). The Spectrotemporal Filter Mechanism of Auditory Selective Attention. Neuron, 77(4), 750–761. https://doi.org/10.1016/j.neuron.2012.11.034

Liu, Y., Dolan, R. J., Kurth-Nelson, Z., & Behrens, T. E. J. (2019). Human Replay Spontaneously Reorganizes Experience. Cell, 178(3), 640-652.e14. https://doi.org/10.1016/j.cell.2019.06.012

Ólafsdóttir, H. F., Bush, D., & Barry, C. (2018). The Role of Hippocampal Replay in Memory and Planning. Current Biology, 28(1), R37–R50. https://doi.org/10.1016/j.cub.2017.10.073

https://doi.org/10.7554/eLife.101511.2.sa0